



**UNIVERSITI PUTRA MALAYSIA**

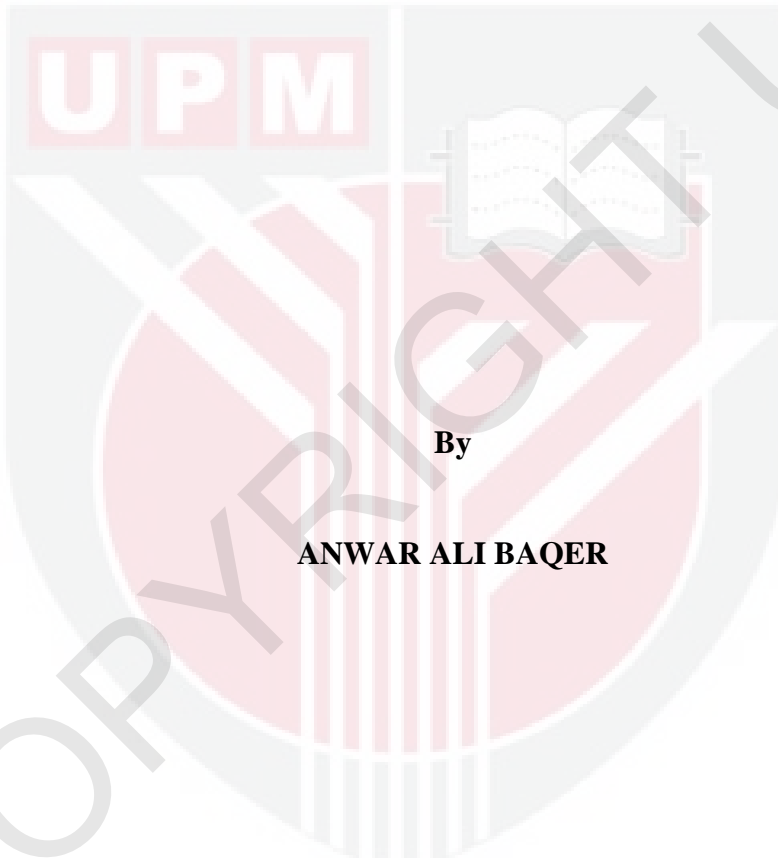
***SYNTHESIS, STRUCTURAL AND OPTICAL CHARACTERIZATION OF  
CuO, CeO<sub>2</sub> AND (CuO)<sub>x</sub>(CeO<sub>2</sub>)<sub>1-x</sub> NANOPARTICLES VIA THERMAL  
TREATMENT METHOD***

**ANWAR ALI BAQER**

**ITMA 2018 5**



**SYNTHESIS, STRUCTURAL AND OPTICAL CHARACTERIZATION OF  
CuO, CeO<sub>2</sub> AND (CuO)<sub>x</sub>(CeO<sub>2</sub>)<sub>1-x</sub> NANOPARTICLES VIA THERMAL  
TREATMENT METHOD**



**Thesis Submitted to the School of Graduate Studies, Universiti of Putra  
Malaysia, in Fulfillment of the Requirements for the Degree of  
Doctor of Philosophy**

**December 2017**

## **COPYRIGHT**

All material contained within the thesis, including without limitation text, logos, icons, photographs and all other artwork, is copyright material of Universiti Putra Malaysia unless otherwise stated. Use may be made of any material contained within the thesis for non-commercial purposes from the copyright holder. Commercial use of material may only be made with the express, prior, written permission of Universiti Putra Malaysia.

Copyright © Universiti Putra Malaysia



## **DEDICATION**

*Finally, a thesis for;*

*My father to whom I am much indebted and my loving mother,  
helpful sisters and brothers.*

*My helpful supervisors, Associate Professor Dr. Khamirul Amin Matori  
for his patience, guidance and encouragement that helped in  
fostering and carrying out this research.*



Abstract of thesis presented to the Senate of Universiti Putra Malaysia in fulfillment  
of the requirements for the degree of Doctor of Philosophy

**SYNTHESIS, STRUCTURAL AND OPTICAL CHARACTERIZATION OF  
CuO, CeO<sub>2</sub> AND (CuO)<sub>x</sub>(CeO<sub>2</sub>)<sub>1-x</sub> NANOPARTICLES VIA THERMAL  
TREATMENT METHOD**

By

**ANWAR ALI BAQER**

**December 2017**

**Chairman : Associate Professor Khamirul Amin Matori, PhD**  
**Institute : Advanced Technology**

Metal oxide semiconductor nanocrystals are regarded as one of the most important inorganic nanomaterials because of their electronic, optical, electrical and magnetic, properties. These properties are dependent on the chemical composition and microstructural characteristics in which the particle size and shape might be controlled in the fabrication processes. Amongst all metal oxide nanoparticles (NPs), copper oxide (CuO), cerium oxide (CeO<sub>2</sub>) and (CuO)<sub>x</sub>(CeO<sub>2</sub>)<sub>1-x</sub> NPs have intriguing properties for the development of novel electronic devices, solar cell, sensor, catalyst and medical applications due to their excellent optical and electronic properties. Therefore, further study is needed to synthesize by other methods and characterize these properties.

CuO, CeO<sub>2</sub> and binary (CuO)<sub>x</sub>(CeO<sub>2</sub>)<sub>1-x</sub> NPs were successfully synthesized by thermal treatment method. The XRD diffraction patterns reveal monoclinic structure for CuO NPs and cubic fluorite structure for CeO<sub>2</sub> NPs. With no other impurities can be detected, indicating the high purity of the final products. The crystallite size was found to increase from 12.64-25.76, 8.71-22.74 and 5.12-15.34 nm for CuO and 6.45-22.18, 7.25-18.76 and 6.15-11.43 nm for CeO<sub>2</sub> with evolution in calcination temperatures 500-800 °C at a concentration of PVP 0.03, 0.04 and 0.05 g/ml respectively. These results were in agreement with the transition electron microscopy results which showed the formation of CuO and CeO<sub>2</sub> in nanoscale size. The average particle size estimated by TEM was found to increase from 15.53 to 30.00 nm, 9.75 to 23.54 nm and 4.25 to 16.93 nm for CuO and 5.15 to 24.19 nm, 4.32 to 20.24 nm and 3.00 to 10.62 nm for CeO<sub>2</sub> with increase in calcination temperature 500-800 °C at a concentration of PVP 0.03, 0.04 and 0.05 g/ml respectively. The FTIR results confirmed the removal of polymer and the presence of metal oxides nanoparticles at

calcination temperatures 500-800 °C. The elemental composition of the samples obtained by EDX spectroscopy has further evidenced the formation highly pure CuO and CeO<sub>2</sub> NPs. Furthermore, the optical band gap of the samples was calculated using Kubelka-Munk function for calcination temperatures 500-800 °C. The band gap was found to decrease from 2.56 to 2.34 eV, 2.75 to 2.42 eV and 2.78 to 2.46 eV for CuO and 3.37 to 3.31eV, 3.38 to 3.32 eV and 3.45 to 3.41 eV for CeO<sub>2</sub> at a concentration of PVP 0.03, 0.04 and 0.05 g/ml respectively. A reduction in the energy band gap with increasing calcination temperatures is attributed to the increase in the particle size. The PL spectra at calcination temperatures 500-800 °C showed that the increment in the intensity with increasing calcination temperatures is attributed to the expansion in the particle size. Due to the control over particle sizes of CuO and CeO<sub>2</sub> that this technique allows by the varying of PVP concentration and calcination temperature, semiconductor materials with wide band gaps can be produced. These materials are able to absorb UV-visible wavelengths of solar energy, making them suitable for use within solar cell applications. Furthermore, CeO<sub>2</sub> materials produced by this method may be acceptable for use in manufacturing UV filters, catalysts and photoelectric devices.

From the XRD diffraction patterns results, the prepared (CuO)<sub>x</sub>(CeO<sub>2</sub>)<sub>1-x</sub> NPs at different calcination temperatures range from 500-800 °C showed that the crystallite size was increased in the range of 11.25-34.17 nm for (CuO)<sub>0.6</sub>(CeO<sub>2</sub>)<sub>0.4</sub> with monoclinic and cubic fluorite structures together with no other impurities can be detected, indicating the high purity of the final products. These results were in agreement with the transition electron microscopy results which showed the formation of (CuO)<sub>x</sub>(CeO<sub>2</sub>)<sub>1-x</sub> in nanoscale size. The average particle size determined by TEM was found to increase 11.96-31.83 nm for (CuO)<sub>0.8</sub>(CeO<sub>2</sub>)<sub>0.2</sub> and 2.97-10.70 nm for (CuO)<sub>0.2</sub>(CeO<sub>2</sub>)<sub>0.8</sub> with increase in calcination temperature 500-800 °C respectively. At the lower concentration of CuO and with calcination temperature, the particle size smaller and consistent for binary (CuO)<sub>x</sub>(CeO<sub>2</sub>)<sub>1-x</sub>. The FTIR results confirmed the removal of polymer and the presence of metal oxide nanoparticles at calcination temperatures 500-800 °C. The elemental composition of the samples obtained by EDX spectroscopy has further evidenced the formation of (CuO)<sub>x</sub>(CeO<sub>2</sub>)<sub>1-x</sub> nanoparticles. In addition, the optical band gap of the samples was calculated using Kubelka-Munk function for calcination temperatures 500-800 °C. The band gap was found to decrease from in the range of 2.82, 3.22 to 2.72, 3.13 eV for (CuO)<sub>0.8</sub>(CeO<sub>2</sub>)<sub>0.2</sub> and 2.90, 3.30 to 2.83, 3.24 eV for (CuO)<sub>0.2</sub>(CeO<sub>2</sub>)<sub>0.8</sub>. A decrease in the energy band gap with increasing calcination temperatures is attributed to the increase in the particle size. The PL spectra at calcination temperatures 500-800 °C showed that the increment in the intensity with increasing calcination temperatures is attributed to the increase in the particle size. Due to the control over (CuO)<sub>x</sub>(CeO<sub>2</sub>)<sub>1-x</sub> particle sizes that this technique allows by the varying of PVP concentration and calcination temperature, semiconductor materials with multiple band gaps can be produced. These materials are able to absorb specific wavelengths of solar energy, making them very suitable for use within solar cell and sensor applications.

Abstrak tesis yang dikemukakan kepada Senat Universiti Putra Malaysia sebagai memenuhi keperluan untuk ijazah Doktor Falsafah

**PENCIRIAN SINTESIS, STRUKTUR DAN OPTIK PARTIKEL NANO CuO,  
CeO<sub>2</sub> DAN (CuO)<sub>x</sub>(CeO<sub>2</sub>)<sub>1-x</sub> MELALUI KAEDAH RAWATAN TERMAL**

Oleh

**ANWAR ALI BAQER**

**Disember 2017**

**Pengerusi : Profesor Madya Khamirul Amin Matori, PhD  
Institut : Teknologi Maju**

Habur nano semikonduktor oksida logam dianggap sebagai salah satu bahan nano tak organik yang paling penting kerana ciri-ciri elektronik, optik, elektrik dan magnetik mereka. Ciri-ciri ini bergantung kepada komposisi kimia dan ciri-ciri mikrostruktur di mana saiz dan bentuk zarah mungkin boleh dikawal dalam proses fabrikasi. Antara bahan zarah nano (NPs) oksida logam, oksida tembaga (CuO), cerium oxide (CeO<sub>2</sub>) dan (CuO)<sub>x</sub>(CeO<sub>2</sub>)<sub>1-x</sub> NPs mempunyai ciri-ciri menarik untuk pembangunan peranti elektronik novel, sel suria, sensor, pemangkin dan aplikasi perubatan disebabkan oleh sifat optik dan elektronik mereka yang sangat baik. Oleh itu, kajian lanjut diperlukan untuk mensintesikan menggunakan kaedah lain dan mencirikan sifat-sifat ini.

CuO, CeO<sub>2</sub> dan dedua (CuO)<sub>x</sub>(CeO<sub>2</sub>)<sub>1-x</sub> NPs telah berjaya disintesis oleh kaedah rawatan haba. Corak pembelauan XRD mendedahkan struktur monoklinik untuk CuO NPs dan struktur fluorit padu untuk CeO<sub>2</sub> NPs. Tanpa sebarang bendasing lain dapat dikesan, menunjukkan ketulenan tinggi bagi produk akhir. Saiz kristal didapati meningkat dari 12.64-25.76, 8.71-22.74 dan 5.12-15.34 nm untuk CuO dan 6.45-22.18, 7.25-18.76 dan 6.15-11.43 nm untuk CeO<sub>2</sub> dengan evolusi dalam suhu kalsinasi 500-800 °C masing-masing pada kepekatan PVP 0.03, 0.04 dan 0.05 g/ml. Keputusan ini sepadan dengan hasil mikroskopi elektron peralihan yang menunjukkan pembentukan CuO dan CeO<sub>2</sub> dalam skala nano saiz. Saiz zarah purata yang dianggarkan oleh TEM dijumpai meningkat dari 15.53 ke 30.00 nm, 9.75 ke 23.54 nm dan 4.25 ke 16.93 nm untuk CuO dan 5.15 ke 24.19 nm, 4.32 ke 20.24 nm dan 3.00 ke 10.62 nm untuk CeO<sub>2</sub> dengan peningkatan suhu kalsinasi 500-800 °C masing-masing pada kepekatan PVP 0.03, 0.04 dan 0.05 g/ml. Hasil FTIR mengesahkan penyingkiran polimer dan kehadiran zarah nano oksida logam pada suhu kalsinasi 500-800 °C. Komposisi unsur sampel yang diperolehi oleh

spektroskopi EDX telah membuktikan pembentukan CuO dan CeO<sub>2</sub> NPs yang sangat tulen. Selain itu, jurang jalur optik sampel dikira menggunakan fungsi Kubelka-Munk untuk suhu kalsinasi 500-800 °C. Jurang jalur didapati menurun dari 2.56 ke 2.34 eV, 2.75 ke 2.42 eV dan 2.78 ke 2.46 eV untuk CuO dan 3.37 ke 3.31eV, 3.38 ke 3.32 eV dan 3.45 ke 3.41 eV untuk CeO<sub>2</sub> masing-masing pada kepekatan PVP 0.03, 0.04 dan 0.05 g/ml. Pengurangan dalam jurang jalur tenaga dengan peningkatan suhu kalsinasi adalah disebabkan peningkatan saiz zarah. Spektrum PL pada suhu kalsinasi 500-800 °C menunjukkan bahawa kenaikan dalam keamatan dengan peningkatan suhu kalsinasi adalah disebabkan oleh peningkatan saiz zarah. Dengan kebolehan pengawalan ke atas saiz zarah CuO dan CeO<sub>2</sub> menggunakan teknik ini dengan mengubah kepekatan PVP dan suhu kalsinasi, bahan semikonduktor dengan jurang lebar boleh dihasilkan. Bahan-bahan ini dapat menyerap panjang gelombang UV tenaga solar, menjadikannya sesuai digunakan dalam aplikasi sel solar. Selain itu, bahan CeO<sub>2</sub> yang dihasilkan menggunakan kaedah ini boleh diterima untuk digunakan dalam pembuatan penapis UV, pemangkin dan peranti fotografi.

Dari hasil corak pembelauan XRD, (CuO)<sub>x</sub>(CeO<sub>2</sub>)<sub>1-x</sub> NPs yang dihasilkan pada suhu kalsinasi berbeza dari 500-800 °C menunjukkan bahawa saiz hablur meningkat dalam lingkungan 11.25-34.17 nm untuk (CuO)<sub>0.6</sub>(CeO<sub>2</sub>)<sub>0.4</sub> dengan struktur fluorit monoklinik dan kubik hadir bersama-sama dengan tiada bendasing lain dapat dikesan, menunjukkan ketulinan tinggi produk akhir. Keputusan ini sepadan dengan hasil mikroskopi elektron peralihan yang menunjukkan pembentukan (CuO)<sub>x</sub>(CeO<sub>2</sub>)<sub>1-x</sub> dalam saiz nano. Saiz zarah purata yang ditentukan oleh TEM didapati meningkat dari 11.96-31.83 nm untuk (CuO)<sub>0.8</sub>(CeO<sub>2</sub>)<sub>0.2</sub> dan 2.97-10.70 nm untuk (CuO)<sub>0.2</sub>(CeO<sub>2</sub>)<sub>0.8</sub> dengan peningkatan suhu kalsinasi masing-masing dari 500-800 °C. Pada kepekatan CuO dan suhu kalsinasi yang rendah, hampir kesemua saiz zarah mengecil dan konsisten bagi binari (CuO)<sub>x</sub>(CeO<sub>2</sub>)<sub>1-x</sub>. Hasil FTIR mengesahkan penyingkiran polimer dan kehadiran nanopartikel oksida logam pada suhu kalsinasi 500-800 °C. Komposisi elemen sampel yang diperolehi dari spektroskopi EDX telah membuktikan pembentukan nanopartikel (CuO)<sub>x</sub>(CeO<sub>2</sub>)<sub>1-x</sub>. Di samping itu, jurang jalur optik sampel dikira menggunakan fungsi Kubelka-Munk untuk suhu kalsinasi 500-800 °C. Jurang jalur didapati berkurang dari julat 2.82, 3.22 ke 2.72, 3.13 eV bagi (CuO)<sub>0.8</sub>(CeO<sub>2</sub>)<sub>0.2</sub> dan 2.90, 3.30 ke 2.83, 3.24 eV bagi (CuO)<sub>0.2</sub>(CeO<sub>2</sub>)<sub>0.8</sub>. Penurunan dalam jurang jalur tenaga dengan peningkatan suhu kalsinasi adalah disebabkan peningkatan saiz zarah. Spektrum PL pada suhu kalsinasi 500-800 °C menunjukkan peningkatan intensiti dengan peningkatan suhu kalsinasi adalah disebabkan oleh peningkatan saiz zarah. Disebabkan oleh pengawalan saiz zarah (CuO)<sub>x</sub>(CeO<sub>2</sub>)<sub>1-x</sub> yang diperolehi dari teknik disebabkan oleh penggunaan pelbagai kepekatan PVP dan suhu kalsinasi, bahan-bahan semikonduktor dengan pelbagai jurang jalur boleh dihasilkan. Bahan-bahan ini dapat menyerap panjang gelombang khusus tenaga solar, menjadikannya sangat sesuai digunakan dalam sel solar dan aplikasi sensor.

## **ACKNOWLEDGEMENTS**

All praise to supreme Allah (S.W.T.). The only creator, cherisher, sustainer, and able who gave me the ability to accomplish this project successfully.

First of all, I would like to thank my supervisor, Associate Professor Dr. Khamirul Amin Matori for embarking with me on this project. There is nothing greater than the gift of working in a field one loves, and you allowed for this to happen. This has been an amazing learning experience. Thank you for your time, your invaluable patience to accomplish this work successfully.

I would also like to extend my sincere appreciation to my supervisory committee members Prof. Dr. Abdul Halim Shaari and Dr. Josephine Liew Ying Chyi for their patience, valuable suggestions and support throughout the dissertation accomplishment process.

My profound gratitude goes to deceased Prof. Dr. Mansor Hashim for his countless effort and in my PhD research. May Allah SWT grant him al Jannah Firdaus and may Allah forgive his shortcomings,

My deepest gratitude goes to my Parents, brothers, and sisters for their unflagging love and support throughout my life, this dissertation is simply impossible without you.

Very special thanks to Prof. Dr. Elias Saion, Dr. Naif Mohammed Al-Hada and Sanaa Tareq for their help and encouragement me during my studies.

I would like to express my sincere thanks to Ministry of Higher Education in Iraq for providing me with financial support through full period time to get PhD degree at Universiti Putra Malaysia.

To conclude, I would like to express my thanks to my friends for their love, encouragement, and prayers during my study. Last but not least, I would like to thank the staff and lectures of Universiti Putra Malaysia for their supporting the current research.

I certify that a Thesis Examination Committee has met on 7 December 2017 to conduct the final examination of Anwar Ali Baqer on his thesis entitled "Synthesis, Structural and Optical Characterization of CuO, CeO<sub>2</sub> and (CuO)<sub>x</sub>(CeO<sub>2</sub>)<sub>1-x</sub> Nanoparticles via Thermal Treatment Method" in accordance with the Universities and University Colleges Act 1971 and the Constitution of the Universiti Putra Malaysia [P.U.(A) 106] 15 March 1998. The Committee recommends that the student be awarded the Doctor of Philosophy.

Members of the Thesis Examination Committee were as follows:

**Sidek bin Hj. Ab. Aziz, PhD**

Professor  
Faculty of Science  
Universiti Putra Malaysia  
(Chairman)

**Jumiah binti Hassan, PhD**

Associate Professor  
Faculty of Science  
Universiti Putra Malaysia  
(Internal Examiner)

**Halimah binti Mohamed Kamari, PhD**

Associate Professor  
Faculty of Science  
Universiti Putra Malaysia  
(Internal Examiner)

**Mehmet Ertugrul, PhD**

Professor  
Ataturk University  
Turkey  
(External Examiner)



**NOR AINI AB. SHUKOR, PhD**

Professor and Deputy Dean  
School of Graduate Studies  
Universiti Putra Malaysia

Date: 29 January 2018

This thesis was submitted to the Senate of Universiti Putra Malaysia and has been accepted as fulfillment of the requirement for the degree of Doctor of Philosophy. The members of the Supervisory Committee were as follows:

**Khamirul Amin Matori, PhD**

Associate Professor

Faculty of Science

Universiti Putra Malaysia

(Chairman)

**Abdul Halim Shaari, PhD**

Professor

Faculty of Science

Universiti Putra Malaysia

(Member)

**Josephine Liew Ying Chyi, PhD**

Senior Lecturer

Faculty of Science

Universiti Putra Malaysia

(Member)

---

**ROBIAH BINTI YUNUS, PhD**

Professor and Dean

School of Graduate Studies

Universiti Putra Malaysia

Date:

## **Declaration by graduate student**

I hereby confirm that:

- this thesis is my original work;
- quotations, illustrations and citations have been duly referenced;
- this thesis has not been submitted previously or concurrently for any other degree at any other institutions;
- intellectual property from the thesis and copyright of thesis are fully-owned by Universiti Putra Malaysia, as according to the Universiti Putra Malaysia (Research) Rules 2012;
- written permission must be obtained from supervisor and the office of Deputy Vice-Chancellor (Research and Innovation) before thesis is published (in the form of written, printed or in electronic form) including books, journals, modules, proceedings, popular writings, seminar papers, manuscripts, posters, reports, lecture notes, learning modules or any other materials as stated in the Universiti Putra Malaysia (Research) Rules 2012;
- there is no plagiarism or data falsification/fabrication in the thesis, and scholarly integrity is upheld as according to the Universiti Putra Malaysia (Graduate Studies) Rules 2003 (Revision 2012-2013) and the Universiti Putra Malaysia (Research) Rules 2012. The thesis has undergone plagiarism detection software.

Signature: \_\_\_\_\_ Date: \_\_\_\_\_

Name and Matric No.: Anwar Ali Baqer, GS 39679

## **Declaration by Members of Supervisory Committee**

This is to confirm that:

- The research conducted and the writing of this thesis was under our supervision;
- Supervision responsibilities as stated in the Universiti Putra Malaysia (Graduate Studies) Rules 2003 (Revision 2012-2013) are adhered to.

Signature:  
Name of  
Chairman of  
Supervisory  
Committee:

Signature:  
Name of  
Member of  
Supervisory  
Committee:

Signature:  
Name of  
Member of  
Supervisory  
Committee:

ASSOC. PROF. DR. KHAMIRUL AMIN MATORI  
Deputy Dean (Development and Finance)  
Faculty of Science  
Universiti Putra Malaysia  
43400 UPM Serdang, Selangor  
Malaysia

Associate Professor Dr. Khamirul Amin Matori

PROF. DR. ABDUL HALIM SHAARI  
Jabatan Fizik  
Fakulti Sains  
Universiti Putra Malaysia  
43400 UPM Serdang,  
Selangor Darul Ehsan, Malaysia

Professor Dr. Abdul Halim Shaari

DR. JOSEPHINE LIEW YING CHYI  
Pensyarah Kanan  
Jabatan Fizik, Fakulti Sains  
Universiti Putra Malaysia  
43400 UPM Serdang

Dr. Josephine Liew Ying Chyi

## TABLE OF CONTENTS

	Page
<b>ABSTRACT</b>	i
<b>ABSTRAK</b>	iii
<b>ACKNOWLEDGEMENTS</b>	v
<b>APPROVAL</b>	vi
<b>DECLARATION</b>	viii
<b>LIST OF TABLES</b>	xiii
<b>LIST OF FIGURES</b>	xv
<b>LIST OF ABBREVIATIONS</b>	xxii
 <b>CHAPTER</b>	
<b>1      INTRODUCTION</b>	 1
1.1     Background of the study	1
1.2     Problem statement	3
1.3     Significance of study	4
1.4     Scope of study	4
1.5     Hypothesis	4
1.6     Objectives of study	5
1.7     Thesis outline	5
<b>2      LITERATURE REVIEW</b>	 6
2.1     Introduction	6
2.2     Methods for synthesis of metal oxide nanoparticles	6
2.2.1     Hydrothermal method	7
2.2.2     Sol-gel method	9
2.2.3     Precipitation method	11
2.2.4     Microwave method	13
2.2.5     Wet chemical method	14
2.2.6     Thermal decomposition method	15
2.2.7     Mechanochemical method	16
2.2.8     Solvothermal method	16
2.2.9     Microemulsion method	18
2.2.10     Sonochemical method	19
2.2.11     Thermal treatment method	20
2.3     Applications of CuO and CeO <sub>2</sub> nanoparticles	25
2.3.1     Sensors applications	25
2.3.2     Solar cells applications	26
2.3.3     Photodetectors applications	26
2.3.4     Catalytic applications	27
2.3.5     Biological and medical applications	28

<b>3</b>	<b>THEORY</b>	29
3.1	Copper oxide (CuO) semiconductor: structure and properties	29
3.2	Cerium oxide (CeO <sub>2</sub> ) semiconductor: structure and properties	30
3.3	Polyvinylpyrrolidone (PVP)	31
3.4	Optical properties of semiconductors	32
3.4.1	Introduction to energy bands	32
3.4.2	Energy band formation	33
3.4.3	Fundamental absorption edge	33
3.4.4	Direct and indirect band gap semiconductor materials	34
3.4.5	Excitonic absorption	35
3.4.6	Density of states and dimensions of material	36
3.4.7	Fermi energy level in semiconductor	38
3.4.8	Quantization in low dimensional structures	41
3.5	Optical emission	43
3.5.1	Generation of electron-hole pairs	43
3.5.2	Recombination mechanism in semiconductor	44
3.5.2.1	Intrinsic recombination	44
3.5.2.2	Radiative band-band recombination	44
3.5.2.3	Extrinsic recombination mechanism	45
<b>4</b>	<b>MATERIALS AND METHOD</b>	47
4.1	Introduction	47
4.2	Materials	47
4.3	Experimental methods	47
4.3.1	Preparation of copper oxide semiconductor nanoparticles	47
4.3.2	Preparation of cerium oxide semiconductor nanoparticles	48
4.3.3	Preparation of binary (CuO) <sub>x</sub> (CeO <sub>2</sub> ) <sub>1-x</sub> semiconductor nanoparticles	48
4.4	Characterizations	50
4.4.1	Thermo-gravimetric analysis (TGA)	50
4.4.2	X-Ray diffraction (XRD)	51
4.4.3	Field emission scanning electron microscopy (FESEM)	53
4.4.4	Transmission electron microscopy (TEM)	54
4.4.5	Fourier transform infrared spectroscopy (FTIR)	55
4.4.6	Energy dispersive X-ray (EDX) spectroscopy	56
4.4.7	UV-Visible spectrophotometer measurement	57
4.4.8	Photoluminescence (PL) measurement	59
<b>5</b>	<b>RESULTS AND DISCUSSION</b>	61
5.1	Introduction	61
5.2	Thermal analysis of CuO, CeO <sub>2</sub> and (CuO) <sub>x</sub> (CeO <sub>2</sub> ) <sub>1-x</sub> nanoparticles	61
5.2.1	TGA-DTG measurement for metal nitrates with PVP	61
5.2.2	TGA-DTG measurements for the bimetal nitrate with PVP	62
5.3	CuO nanoparticles characterization	63
5.3.1	X-Ray diffraction patterns for CuO nanoparticles	63
5.3.2	FESEM micrographs of CuO nanoparticles	68
5.3.3	TEM micrographs of CuO nanoparticles	70

5.3.4	FTIR analysis of CuO nanoparticles	76
5.3.5	EDX analysis of CuO nanoparticles	82
5.3.6	Band gap of CuO nanoparticles	83
5.3.7	PL measurements of CuO nanoparticles	86
5.3.8	Formation mechanism of CuO nanoparticles	89
5.4	CeO <sub>2</sub> nanoparticles characterization	90
5.4.1	X-Ray diffraction eatterns of CeO <sub>2</sub> nanoparticles	90
5.4.2	FESEM micrographs of CeO <sub>2</sub> nanoparticles	95
5.4.3	TEM micrographs of CeO <sub>2</sub> nanoparticles	96
5.4.4	FTIR analysis of CeO <sub>2</sub> nanoparticles	103
5.4.5	EDX analysis of CeO <sub>2</sub> nanoparticles	110
5.4.6	Band gap of CeO <sub>2</sub> nanoparticles	110
5.4.7	PL measurements of CeO <sub>2</sub> nanoparticles	113
5.4.8	Formation mechanism of CeO <sub>2</sub> nanoparticles	116
5.5	Characterization of (CuO) <sub>x</sub> (CeO <sub>2</sub> ) <sub>1-x</sub> nanoparticles	117
5.5.1	X-Ray diffraction patterns of binary (CuO) <sub>x</sub> (CeO <sub>2</sub> ) <sub>1-x</sub> nanoparticles	117
5.5.2	FESEM morphologies of binary (CuO) <sub>x</sub> (CeO <sub>2</sub> ) <sub>1-x</sub> nanoparticles	119
5.5.3	TEM micrographs of binary (CuO) <sub>x</sub> (CeO <sub>2</sub> ) <sub>1-x</sub> nanoparticles	122
5.5.4	FTIR spectra of binary (CuO) <sub>x</sub> (CeO <sub>2</sub> ) <sub>1-x</sub> nanoparticles	128
5.5.5	EDX spectra of binary (CuO) <sub>x</sub> (CeO <sub>2</sub> ) <sub>1-x</sub> nanoparticles	129
5.5.6	Band gap of binary (CuO) <sub>x</sub> (CeO <sub>2</sub> ) <sub>1-x</sub> nanoparticles	131
5.5.7	PL measurements of binary (CuO) <sub>x</sub> (CeO <sub>2</sub> ) <sub>1-x</sub> nanoparticles	134
5.5.8	Formation mechanism of binary (CuO) <sub>x</sub> (CeO <sub>2</sub> ) <sub>1-x</sub> nanoparticles	137
<b>6</b>	<b>CONCLUSION AND FUTURE RESEARCH</b>	139
6.1	Conclusion	139
6.2	Recommendations for future research	140
<b>REFERENCES</b>		142
<b>BIODATA OF STUDENT</b>		164
<b>LIST OF PUBLICATIONS</b>		165

## LIST OF TABLES

<b>Table</b>		
2.1 Summary of various methods and materials used to synthesize CuO and CeO <sub>2</sub> NPs	22	
5.1 Average crystallite size of CuO NPs synthesized at different PVP concentrations and varying calcination temperatures, as determined from XRD results	68	
5.2 Average particle size of CuO NPs synthesized with varying PVP concentrations and different calcination temperatures, as determined from TEM images	76	
5.3 Absorption frequencies and assignment for CuO NPs prepared without using PVP obtained from FTIR spectra	78	
5.4 Absorption frequencies and assignment for CuO NPs at varied PVP concentration obtained from FTIR spectra	82	
5.5 Energy gap of CuO NPs prepared at different calcination temperatures and various concentrations of PVP	86	
5.6 Intensities values of CuO NPs powder prepared at different calcination temperatures and varying PVP concentrations obtained from PL spectra	89	
5.7 Average crystallite size of CeO <sub>2</sub> NPs synthesized at different PVP concentrations and varying calcination temperatures, as determined from XRD results	94	
5.8 Average particle size of CeO <sub>2</sub> NPs synthesized with varying PVP concentrations and different calcination temperatures, as determined from TEM	103	
5.9 Absorption frequencies and assignment for CeO <sub>2</sub> NPs prepared without using PVP obtained from FTIR spectra	105	
5.10 Absorption frequencies and assignment for CeO <sub>2</sub> NPs at varied PVP concentration which obtained from FTIR spectra	109	
5.11 Energy gap of CeO <sub>2</sub> NPs prepared at different calcination temperatures and various PVP concentrations	113	
5.12 Intensities values of CeO <sub>2</sub> NPs powder prepared at different calcination temperatures and varying PVP concentrations obtained from PL spectra	116	

5.13	Average particle size of $(\text{CuO})_x(\text{CeO}_2)_{1-x}$ NPs synthesized at different calcination temperatures, as determined from TEM images	128
5.14	Absorption frequencies and assignment for $(\text{CuO})_{0.6}(\text{CeO}_2)_{0.4}$ NPs at 0.4 g/ml of PVP concentration obtained from FTIR spectra	129
5.15	Atomic percentage of Cu, Ce, and O in $(\text{CuO})_x(\text{CeO}_2)_{1-x}$ NPs obtained from EDX data	130
5.16	Energy gap of $(\text{CuO})_x(\text{CeO}_2)_{1-x}$ NPs powder as a function of x alongside with $E_g$ of CuO and CeO <sub>2</sub> NPs	134
5.17	Intensities values of $(\text{CuO})_x(\text{CeO}_2)_{1-x}$ NPs powder as a function of x at various calcination temperatures obtained from PL spectra	137

## LIST OF FIGURES

Figure	Page
1.1 Relationship between particle size and surface area (Meşin, 2012)	1
1.2 A schematic representation of excited states available to valance electrons (Archana, 2011)	2
2.1 Two integral approaches to the nanomaterials preparation (Dodoo-Arhin, 2010)	7
3.1 Crystal structure of copper oxide (CuO). The blue spheres represent Cu atoms and red spheres represent O atoms (Moreno et al., 2014)	29
3.2 Crystal structure of cerium oxide ( $\text{CeO}_2$ ). Red and white balls indicate O and Ce atoms, respectively (Graciani et al., 2010)	30
3.3 Molecular structure of poly(vinylpyrrolidone) (PVP) ( $\text{C}_6\text{H}_9\text{NO}_n$ ) (Negahdary et al., 2012)	31
3.4 Illustration of the formation of energy bands in a Si crystal (Razeghi, 2009)	32
3.5 Energy band gap diagram of (a) direct band gap semiconductor and (b) indirect band gap semiconductor (Kittel, 2005)	34
3.6 Schematic illustration of excitonic bands for $n = 1$ and 2 in semiconductors. $E_g$ represents the energy gap (Singh, 2006)	36
3.7 The relationship between the density of states and the system dimension (Han, 2008)	38
3.8 Fermi–Dirac distribution functions at $T = 0$ K and at two $T > 0$ K (Tang, 2005)	39
3.9 Different types of nanostructures: (a) a quantum well, (b) a quantum wire, and (c) a quantum dot (Mitin et al., 2010)	41
3.10 Energy levels in quantum dots (Mitin et al., 2010)	43
3.11 Schematic diagram of intrinsic recombination mechanisms: (a) radiative band-band recombination and (b) Auger band-band recombination (Rein, 2005)	45
4.1 Flowchart of the synthesis of metal oxide nanoparticles by thermal treatment method	49

4.2	Simplified representation of the TGA instrument	51
4.3	Simplified illustration of an X-ray diffractometer (Cullity, 1978)	52
4.4	Simplified representation of FSEM (Voutou et al., 2008)	53
4.5	Simplified representation of TEM (Brian et al., 2011)	54
4.6	Simplified representation of FTIR instrument (Pavia, 2001)	56
4.7	Simplified representation of EDX spectrometer and related electronics (Soltani, 2012)	57
4.8	Simplified representation of the UV-Visible spectroscopy procedure (Smith, 1978)	58
4.9	Typical experiment set-up for measurements (Soltani, 2012)	59
5.1	Thermogravimetric analysis (TGA) and thermogravimetric derivative (DTG) curves for the metal nitrates with PVP at the heating rate of 10 °C/ min	62
5.2	Thermogravimetric analysis (TGA) and thermogravimetric derivative (DTG) curves for copper and cerium nitrate with PVP at the heating rate of 10 °C/ min	63
5.3	XRD patterns of CuO NPs prepared without using PVP, at different calcination temperatures (a) R.T., (b) 500, (c) 600, (d) 700 and (e) 800 °C	64
5.4	XRD patterns of CuO NPs synthesized at PVP concentration of 0.03 g/ml, at different calcination temperatures (a) R.T., (b) 500, (c) 600, (d) 700 and (e) 800 °C	66
5.5	XRD patterns of CuO NPs synthesized at PVP concentration of 0.04 g/ml, at different calcination temperatures (a) R.T., (b) 500, (c) 600, (d) 700 and (e) 800 °C	67
5.6	XRD patterns of CuO NPs synthesized at PVP concentration of 0.05 g/ml, at different calcination temperatures (a) R.T., (b) 500, (c) 600, (d) 700 and (e) 800 °C	67
5.7	FESEM micrographs of the CuO NPs prepared without using PVP, at different calcination temperatures (a) 500, (b) 600, (c) 700 and (d) 800 °C	69
5.8	FESEM micrographs of the CuO NPs at 0.04 g/ml PVP, at different calcination temperatures (a) 500, (b) 600, (c) 700 and (d) 800 °C	70

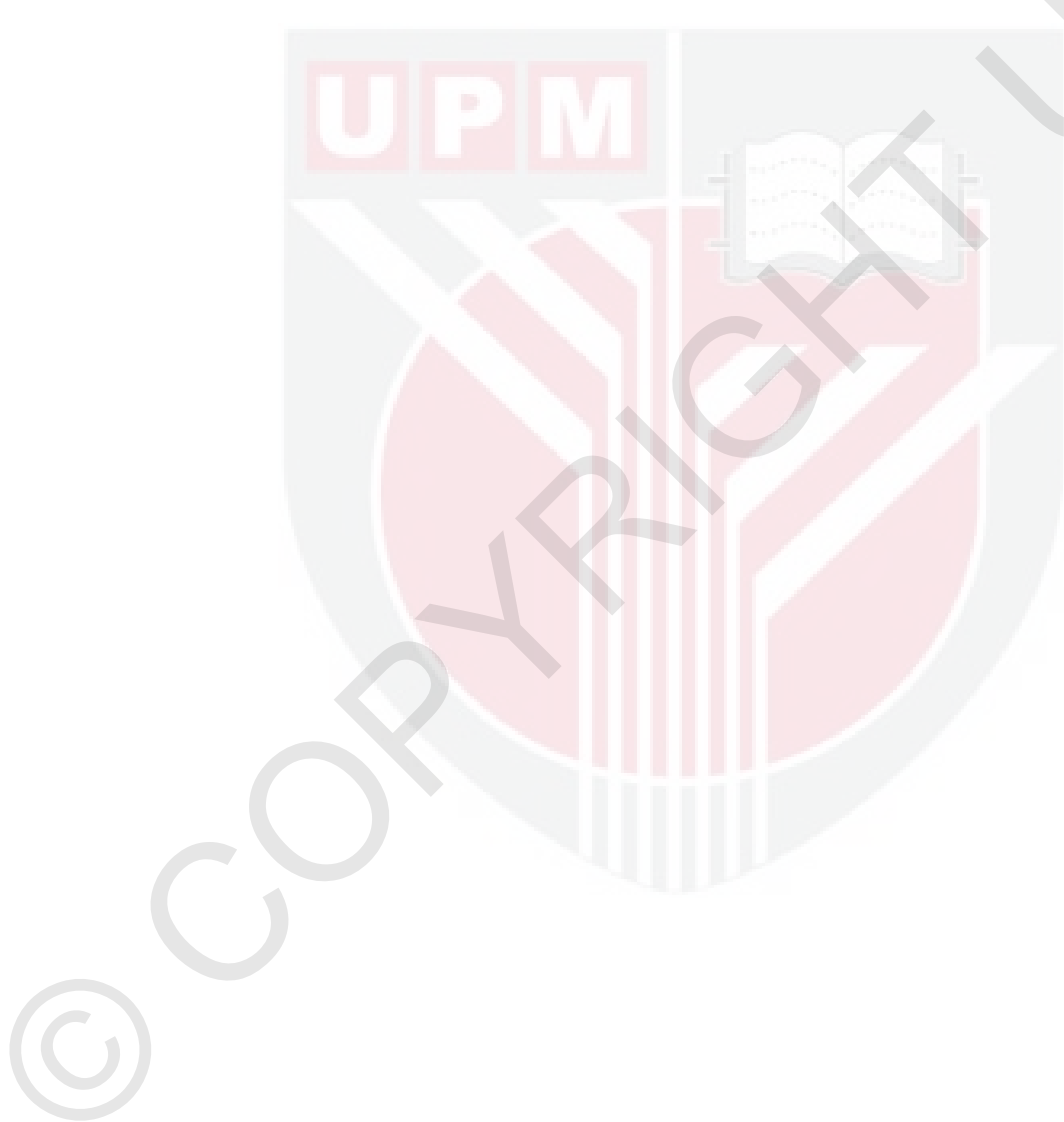
5.9	TEM micrographs of the CuO NPs prepared without using PVP, at different calcination temperatures (a) 500, (b) 600, (c) 700 and (d) 800 °C	71
5.10	TEM micrographs and related size distribution histogram of CuO NPs at 0.03 g/ml of PVP, at different calcination temperatures (a) 500, (b) 600, (c) 700 and (d) 800 °C	72
5.11	TEM micrographs and related size distribution histogram of CuO NPs at 0.04 g/ml of PVP, at different calcination temperatures (a) 500, (b) 600, (c) 700 and (d) 800 °C	74
5.12	TEM micrographs and related size distribution histogram of CuO NPs at 0.05 g/ml of PVP, at different calcination temperatures (a) 500, (b) 600, (c) 700 and (d) 800 °C	75
5.13	FTIR spectra of CuO NPs prepared without using PVP and calcined at varying temperatures (a) R.T., (b) 500, (c) 600, (d) 700 and (e) 800 °C	78
5.14	FTIR spectra of CuO NPs prepared at 0.03 g/ml of PVP concentration and calcined at varying temperatures (a) R.T., (b) 500, (c) 600, (d) 700 and (e) 800 °C	79
5.15	FTIR spectra of CuO NPs prepared at 0.04 g/ml of PVP concentration and calcined at varying temperatures (a) R.T., (b) 500, (c) 600, (d) 700 and (e) 800 °C	81
5.16	FTIR spectra of CuO NPs prepared at 0.05 g/ml of PVP concentration and calcined at varying temperatures (a) R.T., (b) 500, (c) 600, (d) 700 and (e) 800 °C	81
5.17	EDX spectrum of CuO NPs calcined at 600 °C	83
5.18	Plot of the square of Kubelka-Munk function versus photon energy for CuO NPs at varying calcination temperatures (a) 500, (b) 600, (c) 700 and (d) 800 °C at 0.03 g/ml of PVP	84
5.19	Plot of the square of Kubelka-Munk function versus photon energy for CuO NPs at varying calcination temperatures (a) 500, (b) 600, (c) 700 and (d) 800 °C at 0.04 g/ml of PVP	85
5.20	Plot of the square of Kubelka-Munk function versus photon energy for CuO NPs at varying calcination temperatures (a) 500, (b) 600, (c) 700 and (d) 800 °C at 0.05 g/ml of PVP	85
5.21	PL spectra of CuO-NPs prepared at different calcination temperatures (a) 500, (b) 600, (c) 700 and (d) 800 °C and different PVP concentrations	88

5.22	The suggested mechanism through which metallic ions interact with PVP	90
5.23	XRD patterns of CeO <sub>2</sub> NPs prepared without using PVP, at different calcination temperatures (a) R.T., (b) 500, (c) 600, (d) 700 and (e) 800 °C	91
5.24	XRD patterns of CeO <sub>2</sub> NPs synthesised at PVP concentration of 0.03 g/ml, at different calcination temperatures (a) R.T., (b) 500, (c) 600, (d) 700 and (e) 800 °C	92
5.25	XRD patterns of CeO <sub>2</sub> NPs synthesised at PVP concentration of 0.04 g/ml, at different calcination temperatures (a) R.T., (b) 500, (c) 600, (d) 700 and (e) 800 °C	93
5.26	XRD patterns of CeO <sub>2</sub> NPs synthesised at PVP concentration of 0.05 g/ml, at different calcination temperatures (a) R.T., (b) 500, (c) 600, (d) 700 and (e) 800 °C	94
5.27	FESEM micrographs of CeO <sub>2</sub> NPs prepared without using PVP, at different calcination temperatures (a) 500, (b) 600, (c) 700 and (d) 800 °C	95
5.28	FESEM micrographs of CeO <sub>2</sub> NPs at 0.04 g/ml PVP, at different calcination temperatures (a) 500, (b) 600, (c) 700 and (d) 800 °C	96
5.29	TEM micrographs of CeO <sub>2</sub> NPs prepared without using PVP, at different calcination temperatures (a) 500, (b) 600, (c) 700 and (d) 800 °C	97
5.30	TEM micrographs and related size distribution histogram of CeO <sub>2</sub> NPs at 0.03 g/ml, at different calcining temperatures (a) 500, (b) 600, (c) 700 and (d) 800 °C	99
5.31	TEM micrographs and related size distribution histogram of CeO <sub>2</sub> NPs at 0.04 g/ml of PVP, at different calcination temperatures (a) 500, (b) 600, (c) 700 and (d) 800 °C	101
5.32	TEM micrographs and related size distribution histogram of CeO <sub>2</sub> NPs at 0.05 g/ml of PVP, at different calcination temperatures (a) 500, (b) 600, (c) 700 and (d) 800 °C	102
5.33 :	FTIR spectra of CeO <sub>2</sub> NPs prepared without using PVP and calcined at varying temperatures (a) R.T., (b) 500, (c) 600, (d) 700 and (e) 800 °C	104
5.34	FTIR spectra of CeO <sub>2</sub> NPs prepared at 0.03 g/ml of PVP concentration and calcined at varying temperatures (a) R.T., (b) 500, (c) 600, (d) 700 and (e) 800 °C	106

5.35	FTIR spectra of CeO <sub>2</sub> NPs prepared at 0.04 g/ml of PVP concentration and calcined at varying temperatures (a) R.T., (b) 500, (c) 600, (d) 700 and (e) 800 °C	107
5.36	FTIR spectra of CeO <sub>2</sub> NPs prepared at 0.05 g/ml of PVP concentration and calcined at varying temperatures (a) R.T., (b) 500, (c) 600, (d) 700 and (e) 800 °C	108
5.37	EDX spectrum of CeO <sub>2</sub> NPs calcined at 600 °C	110
5.38	Plot of the square of Kubelka-Munk function versus photon energy CeO <sub>2</sub> NPs at varying calcination temperatures (a) 500, (b) 600, (c) 700 and (d) 800 °C at 0.03 g/ml of PVP	111
5.39	Plot of the square of Kubelka-Munk function versus photon energy CeO <sub>2</sub> NPs at varying calcination temperatures (a) 500, (b) 600, (c) 700 and (d) 800 °C at 0.04 g/ml of PVP	112
5.40	Plot of the square of Kubelka-Munk function versus photon energy CeO <sub>2</sub> NPs at varying calcination temperatures (a) 500, (b) 600, (c) 700 and (d) 800 °C at 0.05 g/ml of PVP	112
5.41	PL spectra of CeO <sub>2</sub> NPs prepared at different calcination temperatures (a) 500, (b) 600, (c) 700 and (d) 800 °C and different PVP concentrations	115
5.42	Suggested mechanism through which metallic ions interact with PVP	117
5.43	XRD patterns of binary (CuO) <sub>0.6</sub> (CeO <sub>2</sub> ) <sub>0.4</sub> nanoparticles prepared at 0.04 g/ml of PVP with various calcined temperatures at (a) 500 (CuO), (d) 500, (c) 600, (d) 700, (e) 800 °C and (f) 500 (CeO <sub>2</sub> ) °C	118
5.44	FESEM images of binary (CuO) <sub>0.8</sub> (CeO <sub>2</sub> ) <sub>0.2</sub> nanoparticles at 0.04 g/ml of PVP, at calcination temperatures of (a) 500, (b) 600, (c) 700 and (d) 800 °C	119
5.45	FESEM images of binary (CuO) <sub>0.6</sub> (CeO <sub>2</sub> ) <sub>0.4</sub> nanoparticles at 0.04 g/ml of PVP, at calcination temperatures of (a) 500, (b) 600, (c) 700 and (d) 800 °C	120
5.46	FESEM images of binary (CuO) <sub>0.4</sub> (CeO <sub>2</sub> ) <sub>0.6</sub> nanoparticles at 0.04 g/ml of PVP, at calcination temperatures of (a) 500, (b) 600, (c) 700 and (d) 800 °C	121
5.47	FESEM images of binary (CuO) <sub>0.2</sub> (CeO <sub>2</sub> ) <sub>0.8</sub> nanoparticles at 0.04 g/ml of PVP, at calcination temperatures of (a) 500, (b) 600, (c) 700 and (d) 800 °C	122

5.48	TEM images and particle size distribution of $(\text{CuO})_{0.8}(\text{CeO}_2)_{0.2}$ nanoparticles at calcination temperatures of (a) 500, (b) 600, (c) 700 and (d) 800 °C	123
5.49	TEM images and particle size distribution of $(\text{CuO})_{0.6}(\text{CeO}_2)_{0.4}$ nanoparticles at calcination temperatures of (a) 500, (b) 600, (c) 700 and (d) 800 °C	124
5.50	TEM images and particle size distribution of $(\text{CuO})_{0.4}(\text{CeO}_2)_{0.6}$ nanoparticles at calcination temperatures of (a) 500, (b) 600, (c) 700 and (d) 800 °C	125
5.51	TEM images and particle size distribution of $(\text{CuO})_{0.2}(\text{CeO}_2)_{0.8}$ nanoparticles at calcination temperatures of (a) 500, (b) 600, (c) 700 and (d) 800 °C	127
5.52	FTIR spectra of $(\text{CuO})_{0.6}(\text{CeO}_2)_{0.4}$ NPs prepared at 0.04 g/ml of PVP concentration and calcined at varying temperatures (a) R.T., (b) 500, (c) 600, (d) 700 and (e) 800 °C	129
5.53	The EDX spectra of binary $(\text{CuO})_x(\text{CeO}_2)_{1-x}$ NPs at the calcining temperature of 600 °C and at different concentration of precursors (a) $x = 0.8$ , (b) $x = 0.6$ , (c) $x = 0.4$ and (d) $x = 0.2$	130
5.54	Plot of the square of Kubelka-Munk function versus photon energy $(\text{CuO})_{0.8}(\text{CeO}_2)_{0.2}$ NPs at 0.04 g/ml of PVP and at varying calcination temperatures (a) 500, (b) 600, (c) 700 and (d) 800 °C	131
5.55	: Plot of the square of Kubelka-Munk function versus photon energy $(\text{CuO})_{0.6}(\text{CeO}_2)_{0.4}$ NPs at 0.04 g/ml of PVP and at varying calcination temperatures (a) 500, (b) 600, (c) 700 and (d) 800 °C	132
5.56	Plot of the square of Kubelka-Munk function versus photon energy $(\text{CuO})_{0.4}(\text{CeO}_2)_{0.6}$ NPs at 0.04 g/ml of PVP and at varying calcination temperatures (a) 500, (b) 600, (c) 700 and (d) 800 °C	133
5.57	Plot of the square of Kubelka-Munk function versus photon energy $(\text{CuO})_{0.2}(\text{CeO}_2)_{0.8}$ NPs at 0.04 g/ml of PVP and at varying calcination temperatures (a) 500, (b) 600, (c) 700 and (d) 800 °C	133
5.58	PL spectra of $(\text{CuO})_{0.8}(\text{CeO}_2)_{0.2}$ nanoparticles powder, at various calcination temperatures (a) 500, (b) 600, (c) 700 °C and (d) 800 °C at 0.04 g/ml of PVP	135
5.59	PL spectra of $(\text{CuO})_{0.6}(\text{CeO}_2)_{0.4}$ nanoparticles powder, at various calcination temperatures (a) 500, (b) 600, (c) 700 °C and (d) 800 °C at 0.04 g/ml of PVP	135

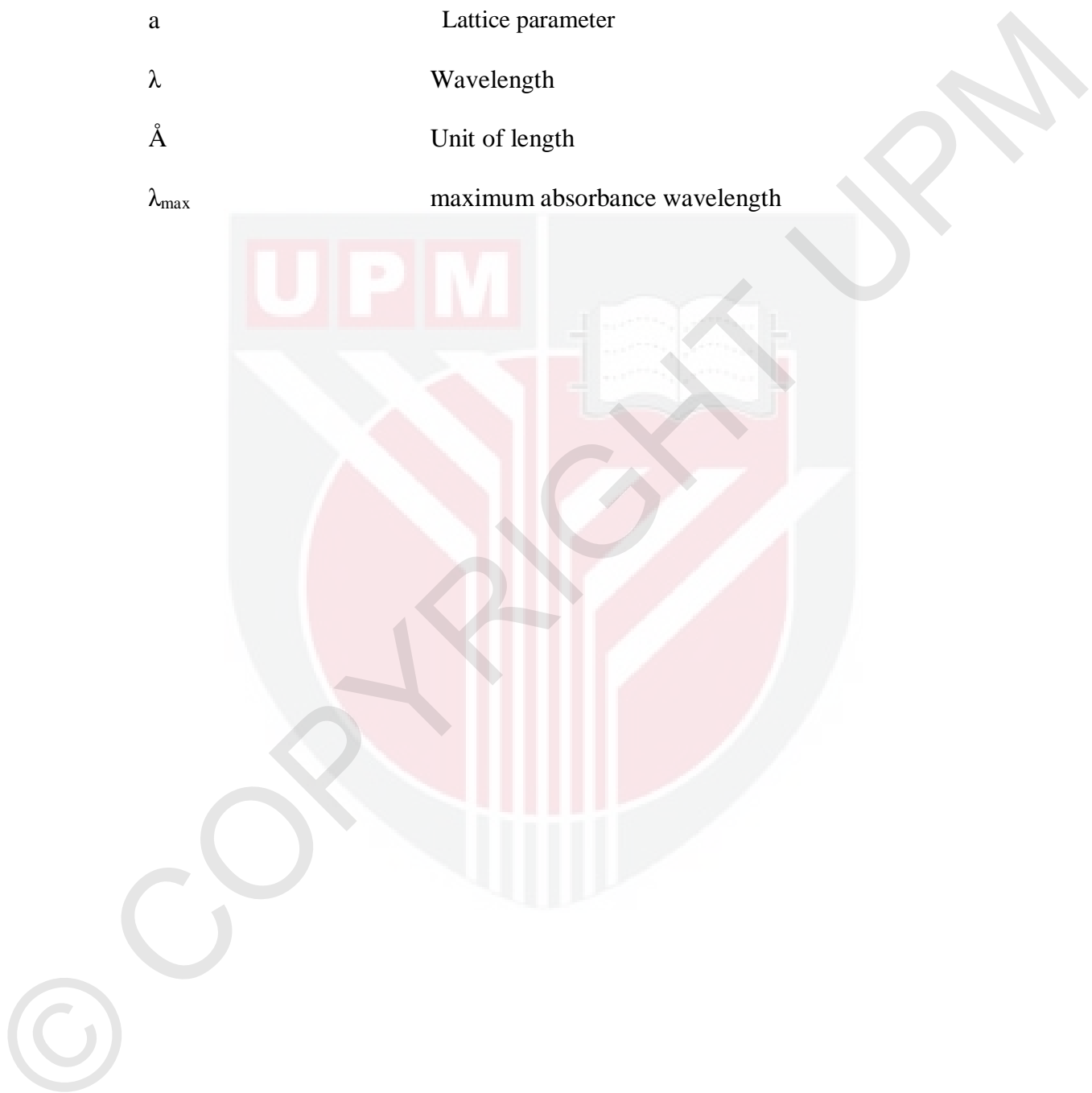
- 5.60 PL spectra of  $(\text{CuO})_{0.4}(\text{CeO}_2)_{0.6}$  nanoparticles powder, at various calcination temperatures (a) 500, (b) 600, (c) 700 °C and (d) 800 °C at 0.04 g/ml of PVP 136
- 5.61 PL spectra of  $(\text{CuO})_{0.2}(\text{CeO}_2)_{0.8}$  nanoparticles powder, at various calcination temperatures (a) 500, (b) 600, (c) 700 °C and (d) 800 °C at 0.04 g/ml of PVP 136
- 5.62 A proposed mechanism of the interaction of the metallic ions and PVP for (a)  $(\text{CuO})_{0.8}(\text{CeO}_2)_{0.2}$ , (b)  $(\text{CuO})_{0.6}(\text{CeO}_2)_{0.4}$ , (c)  $(\text{CuO})_{0.4}(\text{CeO}_2)_{0.6}$  and (d)  $(\text{CuO})_{0.2}(\text{CeO}_2)_{0.8}$  nanoparticles 138



## LIST OF ABBREVIATIONS

A	Absorbance
CCP	Cubic close-packing
CeO <sub>2</sub>	Cerium oxide
CuO	Copper oxide
D	Distance
E <sub>g</sub>	Optical band gap
eV	Electron volte
FESEM	Field emission scanning electron microscopy
FTIR	Fourier transforms infrared spectroscopy
FWHM	Full-width at half-maximum
h	Hour
KM	Kubelka-Munk
min	Minutes
nm	Nanometer
NPs	Nanoparticles
PL	Photoluminescence spectroscopy
PVP	Poly (vinyl pyrrolidone)
R.T.	Room temperature
T	Transmittance
TEM	Transmission electron microscopy
Temp.	Temperature
TGA	Thermo gravimetric analysis
UV-Vis	Ultraviolet-Visible absorption spectroscopy

XRD	X-ray diffraction
$\theta$	Bragg angle
°C	Degree Celsius
a	Lattice parameter
$\lambda$	Wavelength
Å	Unit of length
$\lambda_{\max}$	maximum absorbance wavelength



# CHAPTER 1

## INTRODUCTION

### 1.1 Background of the study

The field of nanotechnology and nanoscience has recently received a growing interest in the literature. The notion of "nanotechnology" was first introduced by Richard Feynman in 1959, in his well-known Caltech lecture titled "there is plenty of room at the bottom: an invitation to enter new field of physics" and made notes on the consequences of measuring and manipulating materials at the nanoscale level. In 1974, Nario Tanigushi coined the term "nanotechnology" and suggested using the name to indicate all the processes that occur in the materials of less than 1 micrometer in size. The prefix "nano" means one-billionth part of something. In general, a nanostructure refers to objects whose size range from individual atoms to a large clusters or molecules (Bardosova and Wagner 2015). The transition of material structure from macroscale to nanoscale results in a dramatic change in the physical, chemical, electrical and optical properties of the new materials. The main reason beyond this change is thought to be due to an increase in the proportion of surface atoms and surface volume ratio, as the size of the particle further decreases.

More importantly, the quantum size effect comes into play when the dimension of the particle is reduced. The carriers (electron-hole) pairs in semiconductor particles are said to be in potential wells defined by the conduction and valence bands of the solid. The quantization effect simply arises from the confinement of charge carriers in semiconductors with potential wells of small dimensions. Depending on the dimensionality of the quantum system, these structures can exist as quantum dots (0-D), quantum wires (1-D) or quantum wells (2-D) (Martienssen and Warlimont, 2005). The relationship between surface area and particle size is inversely proportional with one another (See Figure 1.1).

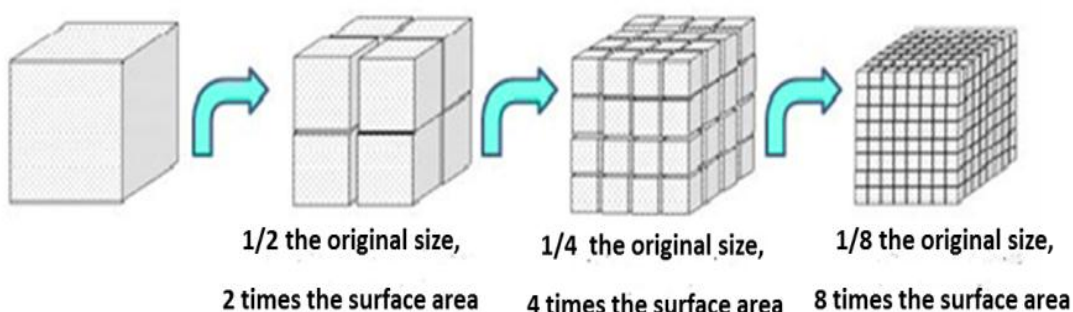


**Figure 1.1 : Relationship between particle size and surface area** (Meşin, 2012)

In confined electronic systems, the size of the particle is comparable to de Broglie wavelength or less; thus, the carrier confinement creates discrete levels in the conduction and valence bands (Grimes et al., 2008). Therfore, the band gap energy and the separation between available states for an excited electron in a nanocrystal become noticeably bigger with diminishing size. This is another particular nanosize impact, wherein, under a specific material based critical size, the electrons in nanocrystal becomes ‘quantum confined’ leading to new size-dependent interactions of the valence electrons to certain energies of excitation (especially photons and electric field) (Archana, 2011).

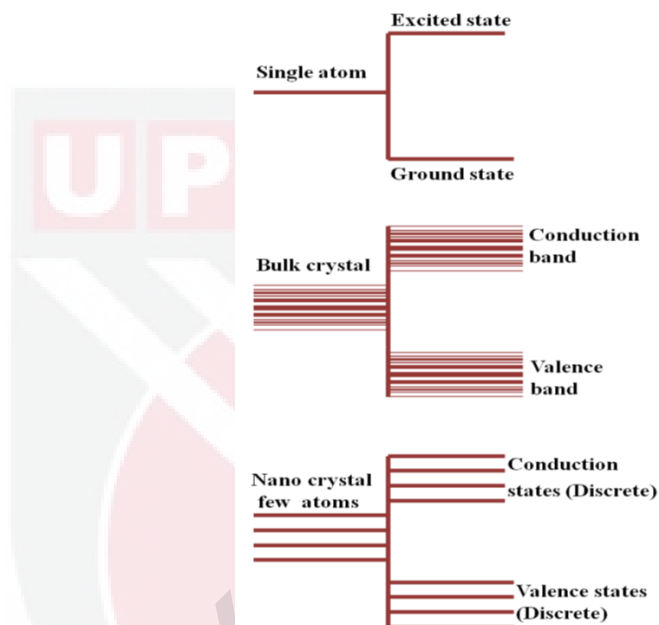


**Figure 1.2 : A schematic representation of excited states available to valence electrons (Archana, 2011)**

The development of nanotechnology has aroused a renewed interest in nanocrystalline materials, which have the ability to improve the properties of the material by controlling the microstructure (Maensiri et al., 2007). Metal oxide nanoparticles and binary oxide nanoparticles are of great interest because of their extensive applications ranging from basic research to applications. For instance, the metal oxide nanoparticles are used in cosmetics, structural materials, biomaterials, paint pigments, electronics, membranes and filters, medical diagnostics, pharmaceuticals, catalysts and supports, flat panel displays, batteries and fuel cells, magnetic and optical devices and in protective coatings (Holmberg, 2001).

## 1.2 Problem statement

Nanoscale metal oxide materials have attracted a lot of researchers attention because of their unique physical and chemical properties depending on their size and dimensionality, as well as their promising applications as key components of micro/nanometric devices. This group has profound applications in areas such as nanophotonics, gas sensor, conversion catalysis and biomedical applications (Mirzaei and Darroudi, 2017; Tyagi et al., 2016). Copper oxide ( $\text{CuO}$ ) and cerium oxide ( $\text{CeO}_2$ ) NPs are considered crucial elements of metal oxide semiconductors due to their p-type and n-type conductivity with band gaps 1.5 eV and 3.2 eV, respectively (Tuller and Nowick, 1979; Mohamed et al., 2014). This renders these materials more appropriate for current technologies.  $\text{CuO}$  and  $\text{CeO}_2$  have potential applications in catalysts (Cao et al., 2008; Lin et al., 2012), gas sensors (Li et al., 2008; Umar et al., 2015), and solar cells (Lira-Cantu and Krebs, 2006; Kidowaki et al., 2011).  $\text{CuO}$  and  $\text{CeO}_2$  NPs have monoclinic and cubic fluorite phases, respectively.

Furthermore, binary  $\text{CuO}-\text{CeO}_2$  NPs semiconductors which consist of two types of materials can usually improve certain functions when compared with their individual components such as catalysis (Chen et al., 2015), water–gas shifts (Li et al., 2007) and solid oxide fuel cell (SOFC) (Ye et al., 2009).

In order to obtain materials with the desired physical and chemical properties, the preparation of the  $\text{CuO}$  and  $\text{CeO}_2$  and binary  $(\text{CuO})(\text{CeO}_2)$  NPs through different methods has become an essential axis of the related research and development activities, namely  $\text{CuO}$  and  $\text{CeO}_2$  NPs such as sol–gel method (Xiao et al., 2009; Mallick and Sahu, 2012), micro emulsion method (Nagy and Dékány, 2009; Zhang et al., 2013), precipitation method (Chung and Yeh, 2008; Phiwdang et al., 2013; Heidari and Irankhah, 2014), thermal decomposition (Zhang et al., 2008c; Gabal et al., 2012), hydrothermal method (Lu et al., 2009; Zeng et al., 2012; Sonia et al., 2015), and solvothermal method (Song et al., 2010; Yu et al., 2012b; Xu et al., 2016). Most of these methods could be used to synthesize nanoparticles of the desired shape and size, but, they are difficult to use on powder form prepared, high purity, a large scale because of their expensive and complex procedures, high reaction temperatures and an addition of toxic reagents which could harm the environment. The thermal treatment method could be deemed as one of the best approaches of forming nanoparticles because it is cheap, fast synthesized pure nanoparticles and also led to an improved characterization of the metal oxide nanoparticles.

Although, many methods could produce copper oxide ( $\text{CuO}$ ) and cerium oxide ( $\text{CeO}_2$ ) nanoparticles separately with small size but to the best of our knowledge until now, none could produce pure binary  $(\text{CuO})_x(\text{CeO}_2)_{1-x}$ nanoparticles in powder form with small size and good distribution of particles. In this method thermal

treatment could produce highly pure binary  $(\text{CuO})_x(\text{CeO}_2)_{1-x}$  nanoparticles in powder form with small particle, narrow size distribution and uniform morphology.

### **1.3 Significance of study**

The metal oxide semiconductors nanoparticles are appealing subjects of constant scientific interest. They have been intensively investigated in the field of materials science, due to their physical-chemical characteristics and their broad range of applications. More specifically, CuO, CeO<sub>2</sub> and binary  $(\text{CuO})_x(\text{CeO}_2)_{1-x}$  NPs semiconductors are usually used as catalytic substances, ultraviolet (UV) filter and absorbents, fuel cells, solar cells, opto-electronic devices, super capacitors, field-emission emitters, sensors, energy storage, electrolyte, biomedical science and several other applications.

In the present study, CuO, CeO<sub>2</sub> and binary  $(\text{CuO})_x(\text{CeO}_2)_{1-x}$  NPs were synthesized from an aqueous mixture containing deionised water, metal nitrates and poly (vinyl pyrrolidone), using a low temperature thermal treatment process. Further processes of grinding and calcinations were applied. No other materials were added to the mixture. This process is eco-friendly in that it neither utilises nor does it create toxic materials, and it offers the benefits of low cost, simplicity, and low reaction temperatures.

### **1.4 Scope of study**

The present research work is limited to the synthesis of CuO, CeO<sub>2</sub> and binary  $(\text{CuO})_x(\text{CeO}_2)_{1-x}$  Nps semiconductors by employing PVP as capping agent, and metal nitrate as precursors through the thermal treatment method. In addition, the study includes structural, morphological and optical characterization of the as-synthesized nanoparticles.

### **1.5 Hypothesis**

The purity of metal oxide nanoparticles produced by thermal treatment method is depended on the interaction between Cu or Ce metallic ions and capping agent (polyvinylpyrrolidone) that undergo to the calcination temperature and causes the growth of the nanoparticles. In this method, the effect of PVP is to establish a distance between the metal atoms, so the agglomeration of oxide particles could be diminished depending upon the PVP concentration. Higher concentration of PVP leads to more capping of metal atoms from each other and manufactured smaller particle size after calcination.

## **1.6 Objectives of study**

The general aim of the present study is to use the thermal treatment method to synthesize CuO, CeO<sub>2</sub> and binary (CuO)<sub>x</sub>(CeO<sub>2</sub>)<sub>1-x</sub> NPs with the aid of PVP acting as a capping agent. It is expected that the nanomaterials synthesized via this technique will improved the physical and chemical properties of the nanoparticles. The specific objectives are stated as follows:

1. To synthesize high purity CuO, CeO<sub>2</sub> and binary (CuO)<sub>x</sub>(CeO<sub>2</sub>)<sub>1-x</sub> NPs via thermal-treatment method.
2. To investigate the effect of calcination temperature on the structural, morphological and optical properties of CuO and CeO<sub>2</sub> NPs.
3. To study the influence of different PVP concentration on the structural, morphological and optical properties of CuO and CeO<sub>2</sub> NPs.
4. To examine the impact of different concentrations of precursor (metal nitrate) and calcination temperatures on the structural, morphological and optical properties of binary (CuO)<sub>x</sub>(CeO<sub>2</sub>)<sub>1-x</sub> NPs semiconductor.

## **1.7 Thesis outline**

This thesis consists of six chapters. Chapter 1 begins with a general introduction of nanotechnology and nanoscience with physical properties of CuO, CeO<sub>2</sub> and binary (CuO)<sub>x</sub>(CeO<sub>2</sub>)<sub>1-x</sub> NPs metal oxides semiconductor. It also discusses the problem statement, research questions and objectives of the study. Chapter 2 provides a comprehensive review of the array of various preparatory techniques used to synthesize CuO, CeO<sub>2</sub> and binary (CuO)<sub>x</sub>(CeO<sub>2</sub>)<sub>1-x</sub> NPs semiconductor with their technological applications. Chapter 3 provides a theoretical background of the present study. This includes the structural, optical, luminescence properties of the as-prepared nanomaterials. Chapter 4 presents the synthesis and characterization of the prepared nanomaterials by thermal treatment method. Chapter 5 presents the results and discussion on the various characterizations of CuO, CeO<sub>2</sub> and binary (CuO)<sub>x</sub>(CeO<sub>2</sub>)<sub>1-x</sub> NPs. Chapter 6 summarizes the study and suggests recommendations for future work.

## REFERENCES

- Agarwal, R., Verma, K., Agrawal, N. K., Duchaniya, R. K., and Singh, R. (2016). (2016). Synthesis, characterization, thermal conductivity and sensitivity of CuO nanofluids. *Applied Thermal Engineering*, 102: 1024-1036.
- Aguirre, J. M., Gutiérrez, A., and Giraldo, O. (2011). Simple route for the synthesis of copper hydroxy salts. *Journal of the Brazilian Chemical Society*, 22(3): 546-551.
- Al-Gaashani, R., Radiman, S., Tabet, N., and Razak Daud, A. (2011). Synthesis and optical properties of CuO nanostructures obtained via a novel thermal decomposition method. *Journal of Alloys and Compounds*, 509(35): 8761-8769.
- Al-Hada, N. M., Saion, E., Kamari, H. M., Flaifel, M. H., Shaari, A. H., Talib, Z. A., Abdullahi, N., Baqer, A. A. and Kharazmi, A. (2016). Structural, morphological and optical behaviour of PVP capped binary  $(\text{ZnO})_{0.4}(\text{CdO})_{0.6}$  nanoparticles synthesised by a facile thermal route. *Materials Science in Semiconductor Processing*, 53: 56-65.
- Al-Hada, N., Saion, E., Talib, Z., and Shaari, A. (2016). The impact of polyvinylpyrrolidone on properties of cadmium oxide semiconductor nanoparticles manufactured by heat treatment technique. *Polymers*, 8(4): 113(1-15).
- Albadi, J., Razeghi, A., Abbaszadeh, H., and Mansournezhad, A. (2013). CuO-CeO<sub>2</sub> Nanocomposite: An Efficient Recyclable Catalyst for the Synthesis of Aryl-14H-dibenzo[a-j]xanthenes. *Journal of Nanoparticles*, 2013: 1-5.
- Alford, T. L., Feldman, L. C., and Mayer, J. W. (2007). Fundamentals of nanoscale film analysis: Springer Science and Business Media.
- Archana, J. (2011). Organic ligand assisted chemical synthesis of ZnSe nanostructures and their functional properties. SRM University.
- Anupriya, K., Vivek, E., and Subramanian, B. (2014). Facile synthesis of ceria nanoparticles by precipitation route for UV blockers. *Journal of Alloys and Compounds*, 590: 406-410.
- Arockiasamy, J. S. K., and Irudayaraj, J. (2016). Natural dye sensitized CuO nanorods for luminescence applications. *Ceramics International*, 42(5): 6198-6205.

- Åsbrink, S., and Norrby, L. J. (1970). A refinement of the crystal structure of copper (II) oxide with a discussion of some exceptional E.s.d.'s. *Acta Crystallographica Section B: Structural Crystallography and Crystal Chemistry*, 26(1): 8-15.
- Ayoman, E., and Hosseini, S. G. (2015). Synthesis of CuO nanopowders by high-energy ball-milling method and investigation of their catalytic activity on thermal decomposition of ammonium perchlorate particles. *Journal of Thermal Analysis and Calorimetry*, 123(2): 1213-1224.
- Azam, A., Ahmed, A. S., Oves, M., Khan, M. S., and Memic, A. (2012). Size-dependent antimicrobial properties of CuO nanoparticles against Gram-positive and -negative bacterial strains. *International Journal of Nanomedicine*, 7: 3527-3535.
- Babitha, K. K., Sreedevi, A., Priyanka, K. P., Sabu, B., and Varghese, T. (2015). Structural characterization and optical studies of CeO<sub>2</sub> nanoparticles synthesized by chemical precipitation. *Indian Journal of Pure and Applied Physics (IJPAP)*, 53(9): 596-603.
- Bardosova, M., and Wagner, T. (2015). Nanomaterials and Nanoarchitectures: A Complex Review of Current Hot Topics and Their Applications: Springer.
- Barreca, D., Bruno, G., Gasparotto, A., Losurdo, M., and Tondello, E. (2003). Nanostructure and optical properties of CeO<sub>2</sub> thin films obtained by plasma-enhanced chemical vapor deposition. *Materials Science and Engineering: C*, 23(6-8): 1013-1016.
- Bharali, D. J., Sahoo, S. K., Mozumdar, S., and Maitra, A. (2003). Cross-linked polyvinylpyrrolidone nanoparticles: a potential carrier for hydrophilic drugs. *Journal of colloid and interface science*, 258(2): 415-423.
- Bhargava, N. N., and Kulshreshtha, D. C., Guptam, S. C. (1984). Basic electronics and linear circuits. Tata McGraw-Hill Education.
- Boldish, S. I., and White, W. B. (1998). Optical band gaps of selected ternary sulfide minerals. *American Mineralogist*, 83(7-8): 865-871.
- Brian J. Ford, D. C. J., Savile Bradbury. (2011). transmission electron microscope (TEM). Encyclopædia Britannica.
- Bruchez, M., Moronne, M., Gin, P., Weiss, S., and Alivisatos, A. P. (1998). Semiconductor nanocrystals as fluorescent Biological Labels. *Science*, 281(5385): 2013-2016.
- Cao, J. L., Shao, G. S., Wang, Y., Liu, Y., and Yuan, Z. Y. (2008). CuO catalysts supported on attapulgite clay for low-temperature CO oxidation. *Catalysis Communications*, 9(15): 2555-2559.

- Celardo, I., Pedersen, J. Z., Traversa, E., and Ghibelli, L. (2011). Pharmacological potential of cerium oxide nanoparticles. *Nanoscale*, 3(4): 1411-1420.
- Chand, P., Gaur, A., and Kumar, A. (2013). Structural, optical and ferroelectric behavior of CuO nanostructures synthesized at different pH values. *Superlattices and Microstructures*, 60: 129-138.
- Chen, G., Xu, Q., Yang, Y., Li, C., Huang, T., Sun, G., Zhang, S., Ma, D. and Li, X. (2015). Facile and Mild Strategy to Construct Mesoporous CeO<sub>2</sub>-CuO Nanorods with Enhanced Catalytic Activity toward CO Oxidation. *ACS Applied Materials and Interfaces*, 7(42): 23538-23544.
- Chen, M. Y., Zu, X. T., Xiang, X., and Zhang, H. L. (2007). Effects of ion irradiation and annealing on optical and structural properties of CeO<sub>2</sub> films on sapphire. *Physica B: Condensed Matter*, 389(2): 263-268.
- Chen, X., and Mao, S. S. (2007). Titanium dioxide nanomaterials: synthesis, properties, modifications, and applications. *Chemical Reviews*, 107(7): 2891-2959.
- Chu, D. Q., Mao, B. G., and Wang, L. M. (2013). Microemulsion-based synthesis of hierarchical 3D flowerlike CuO nanostructures. *Materials Letters*, 105: 151-154.
- Chung, L.-C., and Yeh, C.-T. (2008). Synthesis of highly active CuO-CeO<sub>2</sub> nanocomposites for preferential oxidation of carbon monoxide at low temperatures. *Catalysis Communications*, 9(5): 670-674.
- Comini, E. (2006). Metal oxide nano-crystals for gas sensing. *Analytica chimica acta*, 568(1): 28-40.
- Comini, E., Faglia, G., Sberveglieri, G., Pan, Z., and Wang, Z. L. (2002). Stable and highly sensitive gas sensors based on semiconducting oxide nanobelts. *Applied Physics Letters*, 81(10): 1869-1871.
- Cuenya, B. R. (2010). Synthesis and catalytic properties of metal nanoparticles: Size, shape, support, composition, and oxidation state effects. *Thin Solid Films*, 518(12): 3127-3150.
- Cui, M. Y., Yao, X. Q., Dong, W. J., Tsukamoto, K., and Li, C. R. (2010). Template-free synthesis of CuO-CeO<sub>2</sub> nanowires by hydrothermal technology. *Journal of Crystal Growth*, 312(2): 287-293.
- Cullity, B. D. (1978). Element of X-ray Diffraction (2<sup>nd</sup> ed.). London: Addison-Wesley.
- Czichos H., Saito T., Smith L. R., Smith L (2006). Handbook of materials measurement methods (Vol. 978): Springer.

- Dai, Z. R., Pan, Z. W., and Wang, Z. L. (2002). Growth and structure evolution of novel tin oxide diskettes. *Journal of the American Chemical Society*, 124(29): 8673-8680.
- Darroudi, M., Hakimi, M., Sarani, M., Kazemi Oskuee, R., Khorsand Zak, A., and Gholami, L. (2013). Facile synthesis, characterization, and evaluation of neurotoxicity effect of cerium oxide nanoparticles. *Ceramics International*, 39(6): 6917-6921.
- Devi, A. B., Moirangthem, D. S., Talukdar, N. C., Devi, M. D., Singh, N. R., and Luwang, M. N. (2014). Novel synthesis and characterization of CuO nanomaterials: Biological applications. *Chinese Chemical Letters*, 25(12): 1615-1619.
- Dhineshbabu, N. R., Rajendran, V., Nithyavathy, N., and Vetumperumal, R. (2015). Study of structural and optical properties of cupric oxide nanoparticles. *Applied Nanoscience*, 6(6): 933-939.
- Dodoo-Arhin, D. (2010). Nanostructured Copper Oxide: Production and Application. University of Trento, Italy.
- Dodoo-Arhin, D., Leoni, M., and Scardi, P. (2012). Microemulsion synthesis of copper oxide nanorod-like structures. *Molecular Crystals and Liquid Crystals*, 555(1): 17-31.
- Durran, A. (2000). Quantum Physics of Matter. CRC Press.
- Egerton, R. F. (2005). Physical principles of electron microscopy. New York. Springer.
- Farahmandjou, M., Zarinkamar, M., and Firoozabadi, T. P. (2016). Synthesis of Cerium Oxide ( $\text{CeO}_2$ ) nanoparticles using simple CO-precipitation method. *Revista Mexicana de Física*, 62: 496-499.
- Fterich, M., Nasr, F. B., Lefi, R., Toumi, M., and Guermazi, S. (2016). Effect of concentration of hexamethylenetetramine in structure, microstructure and optical properties of CuO nanoparticles synthesized by hydrothermal route. *Materials Science in Semiconductor Processing*, 43: 114-122.
- Fu, X., Wang, C., Yu, H., Wang, Y., and Wang, T. (2007). Fast humidity sensors based on  $\text{CeO}_2$  nanowires. *Nanotechnology*, 18(14): 145503.
- Gabal, M. A., Elroby, S. A. K., and Obaid, A. Y. (2012). Synthesis and characterization of nano-sized ceria powder via oxalate decomposition route. *Powder Technology*, 229: 112-118.
- Gabbott, P. (2008). Principles and applications of thermal analysis.: John Wiley and Sons.

- Gajendiran, J., and Rajendran, V. (2014). Synthesis and characterization of coupled semiconductor metal oxide (ZnO/CuO) nanocomposite. Materials Letters, 116: 311-313.
- Gajendiran, J., Ramamoorthy, C., Sankar, K. P., Kingsly, T. R. S., Kamalakannan, V., and Krishnamoorthy, T. (2016). Optical and Luminescent Properties of NiO-CuO Nanocomposite by the Precipitation Method. Journal of Advanced Chemical Sciences, 2(2): 227-229.
- Gfroerer, T. H. (2000). Photoluminescence in Analysis of Surfaces and Interfacse. In Encyclopedia of Analytical Chemistry; Meyers, R. A., (Ed.); John Wiley and Sons.
- Gharagozlou, M. (2011). Influence of calcination temperature on structural and magnetic properties of nanocomposites formed by Co-ferrite dispersed in sol-gel silica matrix using tetrakis (2-hydroxyethyl) orthosilicate as precursor. Chemistry Central Journal, 5(1): 19-25.
- Giri, N., Natarajan, R. K., Gunasekaran, S., and Shreemathi, S. (2011).  $^{13}\text{C}$  NMR and FTIR spectroscopic study of blend behavior of PVP and nano silver particles. Archives of Applied Science Research, 3(5): 624-630.
- Gnanam, S., and Rajendran, V. (2010). Synthesis of  $\text{CeO}_2$  or  $\alpha\text{-Mn}_2\text{O}_3$  nanoparticles via sol-gel process and their optical properties. Journal of Sol-Gel Science and Technology, 58(1): 62-69.
- Gomathi, S. S., Nachiyar, G. V., and Nandhini, P. (2016). Effect of Surfactant on the Structural and Optical Properties of CuO Nanoparticles. International Journal of Scientific Research, 5(2): 339-341.
- Graciani, J., Márquez, A. M., Plata, J. J., Ortega, Y., Hernández, N. C., Meyer, A., Zicovich-Wilson, C.M. and Sanz, J. F. (2010). Comparative study on the performance of hybrid DFT functionals in highly correlated oxides: the case of  $\text{CeO}_2$  and  $\text{Ce}_2\text{O}_3$ . Journal of Chemical Theory and Computation, 7(1): 56-65.
- Griffiths, P. R., and De Haseth, J. A. (2007). Fourier transform infrared spectrometry (Vol. 171). John Wiley and Sons.
- Grimes, C. A., Varghese, O. K., and Ranjan, S. (2008). Oxide semiconductors: suspended nanoparticle systems. in light, Water, Hydrogen (pp. 371-426): Springer.
- Guo, L., Tong, F., Liu, H., Yang, H., and Li, J. (2012). Shape-controlled synthesis of self-assembly cubic CuO nanostructures by microwave. Materials Letters, 71: 32-35.

- Gutzow, I. S., Schmelzer, J. W. P. (2013). The vitreous state: thermodynamics, structure, rheology, and crystallization (2<sup>nd</sup> ed.). Berlin, New York: Springer.
- Haaf, F., Sanner, A., and Straub, F. (1985). Polymers of N-vinylpyrrolidone: synthesis, characterization and uses. *Polymer Journal*, 17(1): 143-152.
- Han, T. (2008). Optical Properties of Low Dimensional semiconductor materials. Royal Institute of Technology, Stockholm, Sweden.
- Haruta, M. (2002). Catalysis of gold nanoparticles deposited on metal oxides. *Cattech*, 6(3): 102-115.
- Hashem, M., Saion, E., Al-Hada, N. M., Kamari, H. M., Shaari, A. H., Talib, Z. A., Paiman, S.B. and Kamarudeen, M. A. (2016). Fabrication and characterization of semiconductor nickel oxide (NiO) nanoparticles manufactured using a facile thermal treatment. *Results in Physics*, 6: 1024-1030.
- Hassanzadeh-Tabrizi, S. A., Mazaheri, M., Aminzare, M., and Sadrnezhaad, S. K. (2010). Reverse precipitation synthesis and characterization of CeO<sub>2</sub> nanopowder. *Journal of Alloys and Compounds*, 49(1): 499-502.
- Heidari, F., and Irankhah, A. (2014). Effect of surfactants and digestion time on nano crystalline cerium oxide characteristics synthesized by differential precipitation. *Ceramics International*, 40(8): 12655-12660.
- Holmberg, k. (2001). Handbook of applied surface and colloid chemistry. (Vol. 1-2), John Wiley.
- Hong, Q., Cao, Y., Xu, J., Lu, H., He, J., and Sun, J. L. (2014). Self-powered ultrafast broadband photodetector based on p-n heterojunctions of CuO/Si nanowire array. *ACS Applied Materials and Interfaces*, 6(23): 20887-20894.
- Horiuchi, S., Hanada, T., Izu, N., and Matsubara, I. (2012). Electron microscopy investigations of the organization of cerium oxide nanocrystallites and polymers developed in polyvinylpyrrolidone-assisted polyol synthesis process. *Journal of Nanoparticle Research*, 14(3): 734.
- Hou, J., Yang, Y., Wang, P., Wang, C., Miao, L., Wang, X., Lv, B., You, and G.andLiu, Z. (2017). Effects of CeO<sub>2</sub>, CuO, and ZnO nanoparticles on physiological features of *Microcystis aeruginosa* and the production and composition of extracellular polymeric substances. *Environmental Science and Pollution Research*, 24(1): 226-235.
- Hu, C., Zhu, Q., Chen, L., and Wu, R. (2009). CuO-CeO<sub>2</sub> binary oxide nanoplates: Synthesis, characterization, and catalytic performance for benzene oxidation. *Materials Research Bulletin*, 44(12): 2174-2180.

- Hua, M., Zhang, S., Pan, B., Zhang, W., Lv, L., and Zhang, Q. (2012). Heavy metal removal from water/wastewater by nanosized metal oxides: a review. *Journal of Hazardous Materials*, 211: 317-331.
- Huh, P., Yang, J., and Kim, S. C. (2012). Facile formation of nanostructured 1D and 2D arrays of CuO islands. *RSC Advances*, 2(13): 5491-5494.
- Ibrahim, I. M., Ali, I. M., Dheeb, B. I., Abas, Q., Ramizy, A., Eisa, M., and Aljameel, A. (2017). Antifungal activity of wide band gap Thioglycolic acid capped ZnS: Mn semiconductor nanoparticles against some pathogenic fungi. *Materials Science and Engineering: C*, 73: 665-669.
- Imagawa, H., and Sun, S. (2012). Controlled synthesis of monodisperse CeO<sub>2</sub> nanoplates developed from assembled nanoparticles. *The Journal of Physical Chemistry C*, 116(4): 2761-2765.
- Jalilpour, M., and Fathalilou, M. (2012). Effect of aging time and calcination temperature on the cerium oxide nanoparticles synthesis via reverse co-precipitation method. *International Journal of the Physical Sciences*, 7(6): 944-874.
- Jayakumar, G., Irudayaraj, A. A., Raj, A. D., and Anusuya, M. (2016). Investigation on the preparation and properties of nanostructured cerium oxide. *Nanosystems: Physics, Chemistry, Mathematics*, 7(4): 728-731.
- Jiang, L. C., and Zhang, W. D. (2010). A highly sensitive nonenzymatic glucose sensor based on CuO nanoparticles-modified carbon nanotube electrode. *Biosensors and Bioelectronics*, 25(6): 1402-1407.
- Jiang, T., Wang, Y., Meng, D., Wu, X., Wang, J., and Chen, J. (2014). Controllable fabrication of CuO nanostructure by hydrothermal method and its properties. *Applied Surface Science*, 311: 602-608.
- Johan, M. R., Suan, M. S. M., Hawari, N. L., and Ching, H. A. (2011). Annealing effects on the properties of copper oxide thin films prepared by chemical deposition. *International Journal of Electrochemical Science*, 6: 6094-6104.
- John P. Dakin, R. B., Michel Digonnet, K. S. (2006). *Handbook of optoelectronics*. Taylor and Francis group, New York.
- Jung, H. S., Lee, J. K., Nastasi, M., Lee, S. W., Kim, J. Y., Park, J. S., Hong, K. S. and Shin, H. (2005). Preparation of nanoporous MgO-coated TiO<sub>2</sub> nanoparticles and their application to the electrode of dye-sensitized solar cells. *Langmuir*, 21(23): 10332-10335.
- Kannaki, K., Ramesh, P. S., and Geetha, D. (2012). Hydrothermal synthesis of CuO nanostructure and their characterizations. *International Journal of Scientific and Engineering Research*, 3(9): 1-4.

- Khan, S. B., Faisal, M., Rahman, M. M., and Jamal, A. (2011). Exploration of CeO<sub>2</sub> nanoparticles as a chemi-sensor and photo-catalyst for environmental applications. *Science of the Total Environment*, 409(15): 2987-2992.
- Kidowaki, H., Oku, T., Akiyama, T., Suzuki, A., Jeyadevan, B., and Cuya, J. (2011). fabrication and characterization of CuO-based solar cells. *Journal of Materials Science Research*, 1(1): 138-143
- Kittel, C. (2005). *Introduction to solid state physics* (8<sup>th</sup> ed.): Wiley.
- Ko, H.-H., Yang, G., Cheng, H.-Z., Wang, M.-C., and Zhao, X. (2014). Growth and optical properties of cerium dioxide nanocrystallites prepared by coprecipitation routes. *Ceramics International*, 40(3): 4055-4064.
- Koczkur, K. M., Mourdikoudis, S., Polavarapu, L., and Skrabalak, S. E. (2015). Polyvinylpyrrolidone (PVP) in nanoparticle synthesis. *Dalton Transactions*, 44(41): 17883-17905.
- Koebel, M. M., Jones, L. C., and Somorjai, G. A. (2008). Preparation of size-tunable, highly monodisperse PVP-protected Pt-nanoparticles by seed-mediated growth. *Journal of Nanoparticle Research*, 10(6): 1063-1069.
- Krantz-Rülcker, C., Stenberg, M., Winquist, F., and Lundström, I. (2001). Electronic tongues for environmental monitoring based on sensor arrays and pattern recognition: A Review. *Analytica Chimica Acta*, 426(2): 217-226.
- Kumar, E., Selvarajan, P., and Muthuraj, D. (2013). Synthesis and characterization of CeO<sub>2</sub> nanocrystals by solvothermal route. *Materials Research*, 16(2): 269-276.
- Kumar, S., Srivastava, M., Singh, J., Layek, S., Yashpal, M., Materny, A., and Ojha, A. K. (2015). Controlled synthesis and magnetic properties of monodispersed ceria nanoparticles. *AIP Advances*, 5(2): 027109.
- Lanje, A. S., Sharma, S. J., Pode, R. B., and Ningthoujam, R. S. (2010). Synthesis and optical characterization of copper oxide nanoparticles. *Advances in Applied Science Research*, 1(2): 36-40.
- Lee, P. J., Saion, E., Al-Hada, N. M., and Soltani, N. (2015). A simple up-scalable thermal treatment method for synthesis of ZnO nanoparticles. *Metals*, 5(4): 2383-2392.
- Lee, S. J., and Kriven, W. M. (1998). Crystallization and densification of nano-size amorphous cordierite powder prepared by a PVA solution-polymerization route. *Journal of the American Ceramic Society*, 8(10): 2605-2612.

- Li, L., Zhan, Y., Zheng, Q., Zheng, Y., Lin, X., Li, D., and Zhu, J. (2007). Water–gas shift reaction over aluminum promoted Cu/CeO<sub>2</sub> nanocatalysts characterized by XRD, BET, TPR and Cyclic Voltammetry (CV). *Catalysis Letters*, 118(1-2): 91-97.
- Li, Y., Liang, J., Tao, Z., and Chen, J. (2008). CuO particles and plates: synthesis and gas-sensor application. *Materials Research Bulletin*, 43(8): 2380-2385.
- Li, Y., Tokizono, T., Liao, M., Zhong, M., Koide, Y., Yamada, I., and Delaunay, J. J. (2010). Efficient assembly of bridged  $\beta$ -Ga<sub>2</sub>O<sub>3</sub> nanowires for solar-blind photodetection. *Advanced Functional Materials*, 20(22): 3972-3978.
- Li, Y., Wang, H., Xie, L., Liang, Y., Hong, G., and Dai, H. (2011). MoS<sub>2</sub> nanoparticles grown on graphene: an advanced catalyst for the hydrogen evolution reaction. *Journal of the American Chemical Society*, 133(19): 7296-7299.
- Li, Z., Zhang, H., Zheng, W., Wang, W., Huang, H., Wang, C., MacDiarmid, A.G. and Wei, Y. (2008). Highly sensitive and stable humidity nanosensors based on LiCl doped TiO<sub>2</sub> electrospun nanofibers. *Journal of the American Chemical Society*, 130(15): 5036-5037.
- Liao, L., Zhang, Z., Yan, B., Zheng, Z., Bao, Q., Wu, T., Li, C.M., Shen, Z.X., Zhang, J.X., Gong, H. and Gong, H. (2009). Multifunctional CuO nanowire devices: p-type field effect transistors and CO gas sensors. *Nanotechnology*, 20(8): 085203.
- Liao, M., Alvarez, J., Imura, M., and Koide, Y. (2007). Submicron metal-semiconductor-metal diamond photodiodes toward improving the responsivity. *Applied Physics Letters*, 91(16): 163510(1-3).
- Lim, Y. F., Choi, J. J., and Hanrath, T. (2012). Facile synthesis of colloidal CuO nanocrystals for light-harvesting applications. *Journal of Nanomaterials*, 2012: 1635.
- Lin, C. H., Chen, R. S., Chen, T. T., Chen, H. Y., Chen, Y. F., Chen, K. H., and Chen, L. C. (2008). High photocurrent gain in SnO<sub>2</sub> nanowires. *Applied Physics Letters*, 93(11): 1121.
- Lin, X., Zhou, L., Huang, T., and Yu, A. (2012). Cerium oxides as oxygen reduction catalysts for lithium-air batteries. *International Journal of Electrochemical Scince*, 7: 9550-9559.
- Lira-Cantu, M., and Krebs, F. C. (2006). Hybrid solar cells based on MEH-PPV and thin film semiconductor oxides (TiO<sub>2</sub>, Nb<sub>2</sub>O<sub>5</sub>, ZnO, CeO<sub>2</sub> and CeO<sub>2</sub>–TiO<sub>2</sub>): Performance improvement during long-time irradiation. *Solar Energy Materials and Solar Cells*, 90(14): 2076-2086.

- Liu, B., Yu, S., Wang, Q., Hu, W., Jing, P., Liu, Y., Jia, W., Liu, Y., Liu, L. and Zhang, J., (2013). Hollow mesoporous ceria nanoreactors with enhanced activity and stability for catalytic application. *Chemical Communications*, 49(36): 3757-3759.
- Liu, I. T., Hon, M. H., and Teoh, L. G. (2013). Structure and optical properties of CeO<sub>2</sub> nanoparticles synthesized by precipitation. *Journal of Electronic Materials*, 42(8): 2536-2541.
- Lokteva, I., Radychev, N., Witt, F., Borchert, H., Parisi, J., and Kolny-Olesiak, J. (2010). Surface treatment of CdSe nanoparticles for application in hybrid solar cells: The effect of multiple ligand exchange with pyridine. *The Journal of Physical Chemistry C*, 114(29): 12784-12791.
- Lu, X., Li, X., Chen, F., Ni, C., and Chen, Z. (2009). Hydrothermal synthesis of prism-like mesocrystal CeO<sub>2</sub>. *Journal of Alloys and Compounds*, 476(1-2): 958-962.
- Lu, X., Zhao, Y., and Wang, C. (2005). Fabrication of PbS nanoparticles in polymer-fiber matrices by electrospinning. *Advanced Materials*, 17(20): 2485-2488.
- Luna, I. Z., Hilary, L. N., Chowdhury, A. M. S., Gafur, M. A., Khan, N., and Khan, R. A. (2015). Preparation and characterization of copper oxide nanoparticles synthesized via chemical precipitation method. *Open Access Library Journal*, 2(03): 1-8.
- Luo, Y., and Sun, X. (2007). One-step preparation of poly(vinyl alcohol)-protected Pt nanoparticles through a heat-treatment method. *Materials Letters*, 61(10): 2015-2017.
- Maensiri, S., Labuayai, S., Laokul, P., Klinkaewnarong, J., and Swatsitang, E. (2014). Structure and optical properties of CeO<sub>2</sub> nanoparticles prepared by using lemongrass plant extract solution. *Japanese Journal of Applied Physics*, 53(6S): 1-5.
- Maensiri, S., Masingboon, C., Laokul, P., Jareonboon, W., Promarak, V., Anderson, P. L., and Seraphin, S. (2007). Egg white synthesis and photoluminescence of platelike clusters of CeO<sub>2</sub> nanoparticles. *Crystal Growth and Design*, 7: 950-955.
- Mallakpour, S. (2015). The use of poly(amide-imide)/CuO as a filler for the preparation of poly(vinyl pyrrolidone) nanocomposites: Thermal and morphological studies. *Journal of Composite Materials*, 50(9): 1181-1188.
- Mallick, P., and Sahu, S. (2012). Structure, Microstructure and optical absorption analysis of CuO nanoparticles synthesized by sol-gel route. *Nanoscience and Nanotechnology*, 2(3): 71-74.

- Malynych, S., Luzinov, I., and Chumanov, G. (2002). Poly (vinyl pyridine) as a universal surface modifier for immobilization of nanoparticles. *The Journal of Physical Chemistry B*, 106(6): 1280-1285.
- Martienssen, W. and Warlimont, H. (2005). Springer Handbook of condensed matter and materials data . Springer Science and Business Media.
- Mehdizadeh, R., Saghatforoush, L. A., and Sanati, S. (2013). Synthesis and characterization of  $\beta$ -Co(OH)<sub>2</sub>, CuO and ZnO nanostructures by solvothermal Method without any additive. *Journal of the Chinese Chemical Society*, 60(3): 339-344.
- Meng, F., Gong, J., Fan, Z., Li, H., and Yuan, J. (2016). Hydrothermal synthesis and mechanism of triangular prism-like monocrystalline CeO<sub>2</sub> nanotubes via a facile template-free hydrothermal route. *Ceramics International*, 42(4): 4700-4708.
- Meng, F., Lu, F., Wang, L., Cui, J., and Lü, J. (2012). Novel fabrication and synthetic mechanism of CeO<sub>2</sub> nanorods by a chloride-assisted hydrothermal method. *Science of Advanced Materials*, 4(10): 1018-1023.
- Meng, F., Wang, L., and Cui, J. (2013). Controllable synthesis and optical properties of nano-CeO<sub>2</sub> via a facile hydrothermal route. *Journal of Alloys and Compounds*, 556: 102-108.
- Merrifield, R. C., Wang, Z. W., Palmer, R. E., and Lead, J. R. (2013). Synthesis and characterization of polyvinylpyrrolidone coated cerium oxide nanoparticles. *Environmental science and technology*, 47(21): 12426-12433.
- Meşin, T. (2012). Hydrothermal synthesis and characterization of single crystalline CeO<sub>2</sub> nanoparticles for catalytic applications. Master's thesis, İzmir Institute of Technology, Turkish.
- Mitin, V. V., Sementsov, D. I. and Vagidov, N. Z. (2010). Quantum mechanics for nanostructures. Cambridge University Press, UK.
- Mirzaei, H., and Darroudi, M. (2017). Zinc oxide nanoparticles: Biological synthesis and biomedical applications. *Ceramics International*, 43(1): 907-914.
- Mohamed, R. M., Harraz, F. A., and Shawky, A. (2014). CuO nanobelts synthesized by a template-free hydrothermal approach with optical and magnetic characteristics. *Ceramics International*, 40(1): 2127-2133.
- Morales, A. E., Mora, E. S., and Pal, U. (2007). Use of diffuse reflectance spectroscopy for optical characterization of un-supported nanostructures. *Revista Mexicana de Física*, 53(5), 18-22.

- Moreno, J. L. V., Padama, A. A. B., and Kasai, H. (2014). A density functional theory-based study on the dissociation of NO on a CuO(110) surface. *CrystEngComm*, 16(11), 2260-2265.
- Naatz, H., Lin, S., Li, R., Jiang, W., Ji, Z., Chang, C.H., Köser, J., Thöming, J., Xia, T., Nel, A.E. and Mädler, L., (2017). Safe-by-design CuO nanoparticles via fe-doping, Cu–O bond length variation, and biological assessment in cells and zebrafish embryos. *ACS Nano*, 11(1): 501-515.
- Nagy, K., and Dékány, I. (2009). Preparation of nanosize cerium oxide particles in W/O microemulsions. *Colloids and Surfaces A: Physicochemical and Engineering Aspects*, 345(1-3): 31-40.
- Naseri, M. G., Saion, E. B., Ahangar, H. A., Hashim, M., and Shaari, A. H. (2011). Simple preparation and characterization of nickel ferrite nanocrystals by a thermal treatment method. *Powder Technology*, 212(1): 80-88.
- Naseri, M. G., Saion, E. B., Ahangar, H. A., and Shaari, A. H. (2013). Fabrication, characterization, and magnetic properties of copper ferrite nanoparticles prepared by a simple, thermal-treatment method. *Materials Research Bulletin*, 48(4): 1439-1446.
- Naseri, M. G. K., Halimah Mohamed Dehzangi, Arash Kamalianfar, Ahmad Saion, Elias B. (2015). Fabrication of a novel chromium-iron oxide ( $\text{Cr}_2\text{Fe}_6\text{O}_{12}$ ) nanoparticles by thermal treatment method. *Journal of Magnetism and Magnetic Materials*, 389: 113-119.
- Negahdary, M., Mazaheri, G., Rad, S., Hadi, M., Malekzadeh, R., Saadatmand, M. M., Rezaei-Zarchi, S., Pishbin, F. and Khosravian-hemami, M. (2012). Direct electron transfer of hemoglobin on Manganese III Oxide-Ag nanofibers modified glassy carbon electrode. *International journal of analytical chemistry*, 2012: 37583.
- Niu, H., Yang, Q., and Tang, K. (2006). A new route to copper nitrate hydroxide microcrystals. *Materials Science and Engineering: B*, 135(2): 172-175.
- Panahi-Kalamuei, M., Alizadeh, S., Mousavi-Kamazani, M., and Salavati-Niasari, M. (2015). Synthesis and characterization of  $\text{CeO}_2$  nanoparticles via hydrothermal route. *Journal of Industrial and Engineering Chemistry*, 21: 1301-1305.
- Park, J., Joo, J., Kwon, S. G., Jang, Y., and Hyeon, T. (2007). Synthesis of monodisperse spherical nanocrystals. *Angewandte Chemie International Edition*, 46(25): 4630-4660.
- Patsalas, P., Logothetidis, S., and Metaxa, C. (2002). Optical performance of nanocrystalline transparent ceria films. *Applied Physics Letters*, 81(3): 466-468.

- Patsalas, P., Logothetidis, S., Sygellou, L., and Kennou, S. (2003). Structure-dependent electronic properties of nanocrystalline cerium oxide films. *Physical Review B*, 68(3): 1-17.
- Pavia, D. L., Lampman, G. M., Kriz, G. S., and Vyvyan, J. A. (2008). Introduction to spectroscopy. Cengage Learning. (2008). *Introduction to spectroscopy* (4<sup>th</sup> ed.). Brooks/Cole: Belmont, CA.
- Pavia, D.L., Lampman G.M. and Kriz, G.S. (2001), *Introduction to spectroscopy* (3<sup>rd</sup> ed). USA.
- Peniche, C., Zaldívar, D., Pazos, M., Páz, S., Bulay, A. and Román, J. S. (1993). Study of the thermal degradation of poly (N-vinyl-2-pyrrolidone) by thermogravimetry–FTIR. *Journal of Applied Polymer Science*, 50(3): 485-493.
- Pereira, D. C., Faria, D. L. A. d., and Constantino, V. R. (2006). CuII hydroxy salts: characterization of layered compounds by vibrational spectroscopy. *Journal of the Brazilian Chemical Society*, 17(8): 1651-1657.
- Phiwdang, K., Suphankij, S., Mekprasart, W., and Pecharapa, W. (2013). Synthesis of CuO Nanoparticles by Precipitation Method Using Different Precursors. *Energy Procedia*, 34: 740-745.
- Phoka, S., Laokul, P., Swatsitang, E., Promarak, V., Seraphin, S., and Maensiri, S. (2009). Synthesis, structural and optical properties of CeO<sub>2</sub> nanoparticles synthesized by a simple polyvinylpyrrolidone (PVP) solution route. *Materials Chemistry and Physics*, 115(1): 423-428.
- Phokha, S., Pinitsoontorn, S., Chirawatkul, P., Poo-arporn, Y., and Maensiri, S. (2012). Synthesis, characterization, and magnetic properties of monodisperse CeO<sub>2</sub> nanospheres prepared by PVP-assisted hydrothermal method. *Nanoscale Research Letters*, 7(1): 1-13.
- Ping, Z. H., Nguyen, Q. T., Chen, S. M., Zhou, J. Q., and Ding, Y. D. (2001). States of water in different hydrophilic polymers-DSC and FTIR studies. *Polymer*, 42(20): 8461-8467.
- Pournajaf, R., and Hassanzadeh-Tabrizi, S. A. (2015). Effect of heat treatment on the size, structural and catalytic properties of Al<sub>2</sub>O<sub>3</sub>–CeO<sub>2</sub> nanocomposite powder prepared by microemulsion method. *Journal of Sol-Gel Science and Technology*, 75(2): 360-365.
- Pournajaf, R., Hassanzadeh-Tabrizi, S. A., and Jafari, M. (2014). Reverse microemulsion synthesis of CeO<sub>2</sub> nanopowder using polyoxyethylene(23) lauryl ether as a surfactant. *Ceramics International*, 40(6): 8687-8692.

- Prasal, R., Bella, V. R. (2010). A review on diesel soot emission, its effect and control. *Bulletin of Chemical Reaction Engineering and Catalysis*, 5(2): 69-86.
- Prime, R. B., Bair, H. E., Vyazovkin, S., Gallagher, P. K., and Riga. (2009). Thermogravimetric analysis (TGA). In Menczel, J. D., and Prime, R. B. (Ed.), *Thermal analysis of polymers: Fundamentals and applications* (pp. 241-317). Hoboken, New Jersey, Canada: John Wiley and Sons.
- Qin, J., Lu, J., Cao, M., and Hu, C. (2010). Synthesis of porous CuO-CeO<sub>2</sub> nanospheres with an enhanced low-temperature CO oxidation activity. *Nanoscale*, 2(12): 2739-2743.
- Radhakrishnan, A. A., and Beena, B. B. (2014). Structural and optical absorption analysis of CuO nanoparticles. *Indian Journal of Advances in Chemical Science*, 2: 158-161.
- Razeghi, M. (2009). *Fundamentals of solid state engineering* (3<sup>rd</sup> ed.): Springer.
- Reich, S., Thomsen, C., and Maultzsch, J. (2004). *Carbon nanotubes: basic concepts and physical properties*. Wiley-VCH.
- Rein, S. (2005). *Lifetime Spectroscopy: A Method of Defect Characterization in Silicon for Photovoltaic Applications*: Springer.
- Rout, L., Sen, T. K., and Punniyamurthy, T. (2007). Efficient CuO-nanoparticle-catalyzed C-S cross-coupling of thiols with iodobenzene. *Angewandte Chemie International Edition*, 46(29): 5583-5586.
- Sabbaghan, M., Shahvelayati, A. S., and Madankar, K. (2015). CuO nanostructures: Optical properties and morphology control by pyridinium-based ionic liquids. *Spectrochimica Acta Part A: Molecular and Biomolecular Spectroscopy*, 135: 662-668.
- Sahooli, M., Sabbaghi, S., and Saboori, R. (2012). Synthesis and characterization of mono sized CuO nanoparticles. *Materials Letters*, 81: 169-172.
- Salem, A., Saion, E., Al-Hada, N. M., Mohamed Kamari, H., Shaari, A. H., Abdullah, C. A. C., and Radiman, S. (2017). Synthesis and characterization of CdSe nanoparticles via thermal treatment technique. *Results in Physics*, 7: 1556-1562.
- Sathyamurthy, S., Leonard, K. J., Dabestani, R. T., and Paranthaman, M. P. (2005). Reverse micellar synthesis of cerium oxide nanoparticles. *Nanotechnology*, 16(9): 1960-1964.

- Shahmiri, M., Ibrahim, N. A., Yunus, W. M. Z. W., Shameli, K., Zainuddin, N., and Jahangirian, H. (2013). Synthesis and characterization of CuO nanosheets in polyvinylpyrrolidone by quick precipitation method. Advanced Science, Engineering and Medicine, 5(3): 193-197.
- Shao, H., Huang, Y., Lee, H., Suh, Y. J., and Kim, C. O. (2006). Effect of PVP on the morphology of cobalt nanoparticles prepared by thermal decomposition of cobalt acetate. Current Applied Physics, 6: e195-e197.
- Sharma, A., Kumar, P. S., and Sonia, (2012). Synthesis and characterization of nanomaterials and its applications. Archives of Applied Science Research, 4(6): 2557-2563.
- Sheno, N. N., Morsali, A., and Joo, S. W. (2014). Synthesis CuO nanoparticles from a copper(II) metal-organic framework precursor. Materials Letters, 117: 31-33.
- Shukla, D., Himabindu, K., Chidambaram, K., Deshmukh, K., Ahamed, M. B., and Pasha, S. K. (2015). Synthesis of CeO<sub>2</sub> nanoparticles via solvothermal route and their application in sensors. The National conference on Nanomaterials for Environmental [NCNER-2015]. 8(5): 46-53,
- Siddiqui, H., Qureshi, M. S., and Haque, F. Z. (2014). One-step, template-free hydrothermal synthesis of CuO tetrapods. Optik - International Journal for Light and Electron Optics, 125(17): 4663-4667.
- Siddiqui, H., Qureshi, M. S., and Haque, F. Z. (2016). Surfactant assisted wet chemical synthesis of copper oxide (CuO) nanostructures and their spectroscopic analysis. Optik - International Journal for Light and Electron Optics, 127(5): 2740-2747.
- Singh, J. (2006). Optical properties of condensed matter and applications. John Wiley and Sons.
- Smith, R. A. (1978). Semiconductors (2<sup>nd</sup> ed.). Cambridge University Press, London.
- Soltani, N. (2012). Microwave assisted synthesis and photocatalytic activity of ZnS and CdS quantum dot systems. Universiti Putra Malaysia.
- Soltani, N., Saion, E., Hussein, M. Z., Erfani, M., Rezaee, K., and Bahmanrokh, G. (2012). Phase Controlled Monodispersed CdS Nanocrystals Synthesized in Polymer Solution Using Microwave Irradiation. Journal of Inorganic and Organometallic Polymers and Materials, 22(4): 830-836.
- Song, Y., Wei, J., Yang, Y., Yang, Z., and Yang, H. (2010). Preparation of CeO<sub>2</sub> hollow spheres via a surfactant-assisted solvothermal route. Journal of Materials Science, 45(15): 4158-4162.

- Sonia, S., Poongodi, S., Kumar, P. S., Mangalaraj, D., Ponpandian, N., and Viswanathan, C. (2015). Hydrothermal synthesis of highly stable CuO nanostructures for efficient photocatalytic degradation of organic dyes. *Materials Science in Semiconductor Processing*, 30: 585-591.
- Soren, S., Bessoi, M., and Parhi, P. (2015). A rapid microwave initiated polyol synthesis of cerium oxide nanoparticle using different cerium precursors. *Ceramics International*, 41(6): 8114-8118.
- Studer, A.M., Limbach, L.K., Van Duc, L., Krumeich, F., Athanassiou, E.K., Gerber, L.C., Moch, H. and Stark, W.J. (2010). Nanoparticle cytotoxicity depends on intracellular solubility: comparison of stabilized copper metal and degradable copper oxide nanoparticles. *Toxicology Letters*, 197(3): 169-174.
- Subhan, M. A., Ahmed, T., Awal, M. R., and Kim, B. M. (2015). Structure and photoluminescence studies of CeO<sub>2</sub>•CuAlO<sub>2</sub> mixed metal oxide fabricated by co-precipitation method. *Spectrochimica Acta Part A: Molecular and Biomolecular Spectroscopy*, 135: 466-471.
- Sujana, M. G., Chattopadyay, K. K., and Anand, S. (2008). Characterization and optical properties of nano-ceria synthesized by surfactant-mediated precipitation technique in mixed solvent system. *Applied Surface Science*, 254(22): 7405-7409.
- Szczerba, M., Środoń, J., Skiba, M., and Derkowsk, A. (2010). One-dimensional structure of exfoliated polymer-layered silicate nanocomposites: A polyvinylpyrrolidone (PVP) case study. *Applied Clay Science*, 47(3-4): 235-241.
- Tabatabaei, M., ShaikhaliShahi, R., and Mohammadinasab, R. (2013). Sonochemical preparation and characterization of CeO<sub>2</sub> nanoparticles using polyethylene glycols as a neutral surfactant. *Research on Chemical Intermediates*, 41(1): 113-116.
- Tadjarodi, A., and Imani, M. (2011). Synthesis and characterization of CdO nanocrystalline structure by mechanochemical method. *Materials Letters*, 65(6): 1025-1027.
- Tang., C. L. (2005). Fundamentals of quantum mechanics: for solid state electronics and optics. Cambridge University Press, New York, USA.
- Tao, Y., Wang, H., Xia, Y., Zhang, G., Wu, H., and Tao, G. (2010). Preparation of shape-controlled CeO<sub>2</sub> nanocrystals via microwave-assisted method. *Materials Chemistry and Physics*, 124(1): 541-546.
- Taylor, E., and Webster, T. J. (2011). Reducing infections through nanotechnology and nanoparticles. *International Journal of Nanomedicine*, 6: 1463-1473.

- Tian, W., Zhi, C., Zhai, T., Wang, X., Liao, M., Li, S., Chen, S., Golberg, D. and Bando, Y. (2012). Ultrahigh quantum efficiency of CuO nanoparticle decorated In<sub>2</sub>Ge<sub>2</sub>O<sub>7</sub> nanobelt deep-ultraviolet photodetectors. *Nanoscale*, 4(20): 6318-6324.
- Tiwari, J. N., Tiwari, R. N., and Kim, K. S. (2012). Zero-dimensional, one-dimensional, two-dimensional and three-dimensional nanostructured materials for advanced electrochemical energy devices. *Progress in Materials Science*, 57(4): 724-803.
- Tricoli, A., Righettoni, M., and Teleki, A. (2010). Semiconductor gas sensors: dry synthesis and application. *Angewandte Chemie International Edition*, 49(42): 7632-7659.
- Tsunekawa, S., Wang, J. T., Kawazoe, Y., and Kasuya, A. (2003). Blueshifts in the ultraviolet absorption spectra of cerium oxide nanocrystallites. *Journal of Applied Physics*, 94(5): 3654-3656.
- Tyagi, P., Sharma, A., Tomar, M., and Gupta, V. (2016). Metal oxide catalyst assisted SnO<sub>2</sub> thin film based SO<sub>2</sub> gas sensor. *Sensors and Actuators B: Chemical*, 224: 282-289.
- Tuller, H. L., and Nowick, A. S. (1979). Defect structure and electrical properties of nonstoichiometric CeO<sub>2</sub> single crystals. *Journal of the Electrochemical Society*, 126(2): 209-217.
- Umar, A., Kumar, R., Akhtar, M. S., Kumar, G., and Kim, S. H. (2015). Growth and properties of well-crystalline cerium oxide (CeO<sub>2</sub>) nanoflakes for environmental and sensor applications. *Journal of Colloid and Interface Science*, 454: 61-68.
- Usha, V., Kalyanaraman, S., Thangavel, R., and Vettumperumal, R. (2015). Effect of catalysts on the synthesis of CuO nanoparticles: Structural and optical properties by sol-gel method. *Superlattices and Microstructures*, 86: 203-210.
- Uskoković, V., and Drofenik, M. (2005). Synthesis of materials within reverse micelles. *Surface Review and Letters*, 12(02): 239-277.
- Vijaya, M.S., Rangarajan G. (2004) Material Science, Tata McGraw-Hill, New Delhi.
- Vijayakumar, G., Karthick, S. N., and Subramania, A. (2014). Effect of polyvinylpyrrolidone for the Synthesis of Ceria (CeO<sub>2</sub>) nanoparticles by polyol mediated process. *European Journal of Applied Sciences and Technology [EUJAST]*, 1(1): 11-14.

- Vijayalakshmi, K., and Karthick, K. (2013). High quality ZnO/CuO nanocomposites synthesized by microwave assisted reaction. *Journal of Materials Science: Materials in Electronics*, 25(2): 832-836.
- Voutou, B., Stefanaki, E. C. and Giannakopoulos, K. (2008). Electron microscopy: the basics. *Physics of Advanced Materials Winter School*.
- Wang, C., Yin, H., Dai, S., and Sun, S. (2010). A general approach to noble metal–metal oxide dumbbell nanoparticles and their catalytic application for CO oxidation. *Chemistry of materials*, 22(10): 3277-3282.
- Wang, H., Xu, J. Z., Zhu, J. J., and Chen, H. Y., (2002). Preparation of CuO nanoparticles by microwave irradiation. *Journal of Crystal Growth*, 244(1): 88-94.
- Wang, L., and Meng, F. (2013). Oxygen vacancy and Ce<sup>3+</sup> ion dependent magnetism of monocrystal CeO<sub>2</sub> nanopoles synthesized by a facile hydrothermal method. *Materials Research Bulletin*, 48(9): 3492-3498.
- Wang, S. B., Hsiao, C. H., Chang, S. J., Lam, K. T., Wen, K. H., Hung, S. C., Young, S. J. and Huang, B. R., (2011). A CuO nanowire infrared photodetector. *Sensors and Actuators A: Physical*, 171(2): 207-211.
- Wang, X., Hu, C., Liu, H., Du, G., He, X., and Xi, Y. (2010). Synthesis of CuO nanostructures and their application for nonenzymatic glucose sensing. *Sensors and Actuators B: Chemical*, 144(1): 220-225.
- Wang, X., Rodriguez, J. A., Hanson, J. C., Gamarra, D., Martínez-Arias, A., and Fernández-García, M. (2006). In situ studies of the active sites for the water gas shift reaction over Cu–CeO<sub>2</sub> catalysts: complex interaction between metallic copper and oxygen vacancies of ceria. *The Journal of Physical Chemistry B*, 110(1): 428-434.
- Wei, T. Y., Huang, C. T., Hansen, B. J., Lin, Y. F., Chen, L. J., Lu, S. Y., and Wang, Z. L. (2010). Large enhancement in photon detection sensitivity via Schottky-gated CdS nanowire nanosensors. *Applied Physics Letters*, 96(1): 013508.
- West, A. R. (1984). Solid state chemistry and its applications. John Wiley and Sons: Chichester.
- Wetchakun, K., Samerjai, T., Tamaekong, N., Liewhiran, C., Siriwong, C., Kruefu, V., Wisitsoraat, A., Tuantranont, A. and Phanichphant, S., (2011). Semiconducting metal oxides as sensors for environmentally hazardous gases. *Sensors and Actuators B: Chemical*, 160(1): 580-591.
- Whiffen, D. H. (1971). Accurate molecular geometry. *Chemistry in Britain*, 7(2): 57.

- Whitesides, G. M. (2005). Nanoscience, nanotechnology, and chemistry. *Small*, 1(2): 172-179.
- Wiley, B., Sun, Y., Mayers, B., and Xia, Y. (2005). Shape-controlled synthesis of metal nanostructures: the case of silver. *Chemistry*, 11(2): 454-463.
- Williams, D. B., and Carter, C. B. (1996). The transmission electron microscope. In *Transmission electron microscopy* (pp. 3-17): Springer.
- Wongpisutpaisan, N., Charoensuk, P., Vittayakorn, N., and Pecharapa, W. (2011). Sonochemical synthesis and characterization of copper oxide nanoparticles. *Energy Procedia*, 9: 404-409.
- Wu, M. Z., Liu, Y. M., Dai, P., Sun, Z. Q., Liu and X. S. (2010a). Hydrothermal synthesis and photoluminescence behavior of CeO<sub>2</sub> nanowires with the aid of surfactant PVP. *International Journal of Minerals, Metallurgy, and Materials*, 17(4): 470-474.
- Wu, R., Ma, Z., Gu, Z. and Yang, Y. (2010b). Preparation and characterization of CuO nanoparticles with different morphology through a simple quick-precipitation method in DMAc–water mixed solvent. *Journal of Alloys and Compounds*, 504(1): 45-49.
- Xu, P., Niu, H., Chen, J., Song, J., Mao, C., Zhang, S., Gao, Y. and Chen, C. (2016). Facile synthesis of uniform hierarchical composites CuO-CeO<sub>2</sub> for enhanced dye removal. *Journal of Nanoparticle Research*, 18(12):382.
- Xiao, H., Ai, Z., and Zhang, L. (2009). Nonaqueous sol– gel synthesized hierarchical CeO<sub>2</sub> nanocrystal microspheres as novel adsorbents for wastewater treatment. *The Journal of Physical Chemistry C*, 113(38): 16625-16630.
- Xie Y, Zhang S, Pan B, Lv L, Zhang W (2011). Effect of CdS distribution on the photocatalytic performance of resin-CdS nanocomposites. *Chemical Engineering Journal*, 174(1): 351-356.
- Xu, D., Cheng, F., Lu, Q., and Dai, P. (2014). Microwave enhanced catalytic degradation of methyl orange in aqueous solution over CuO/CeO<sub>2</sub> catalyst in the absence and presence of H<sub>2</sub>O<sub>2</sub>. *Industrial and Engineering Chemistry Research*, 53(7): 2625-2632.
- Xu, P., Niu, H., Chen, J., Song, J., Mao, C., Zhang, S., Gao, Y. and Chen, C., (2016). Facile synthesis of uniform hierarchical composites CuO-CeO<sub>2</sub> for enhanced dye removal. *Journal of Nanoparticle Research*, 18(12):382.
- Xu, X., Wang, Q., Choi, H. C., and Kim, Y. H. (2010). Encapsulation of iron nanoparticles with PVP nanofibrous membranes to maintain their catalytic activity. *Journal of Membrane Science*, 348(1-2): 231-237.

- Yadav, T. P., and Srivastava, O. N. (2012). Synthesis of nanocrystalline cerium oxide by high energy ball milling. *Ceramics International*, 38(7): 5783-5789.
- Yang, W., Guo, W., Chang, J., and Zhang, B. (2017). Protein/peptide-templated biomimetic synthesis of inorganic nanoparticles for biomedical applications. *Journal of Materials Chemistry B*, 5(3): 401-417.
- Yao, Y., Liang, Y., Shrotriya, V., Xiao, S., Yu, L. and Yang, Y. (2007). Plastic Near-Infrared Photodetectors Utilizing Low Band Gap Polymer. *Advanced Materials*, 19(22): 3979-3983.
- Ye, X.-F., Wang, S. R., Hu, Q., Chen, J. Y., Wen, T. L., and Wen, Z. Y. (2009). Improvement of Cu–CeO<sub>2</sub> anodes for SOFCs running on ethanol fuels. *Solid State Ionics*, 180(2-3): 276-281.
- You, J., Chen, C.C., Dou, L., Murase, S., Duan, H.S., Hawks, S.A., Xu, T., Son, H.J., Yu, L., Li, G. and Yang, Y., (2012). Metal oxide nanoparticles as an electron-transport layer in high-performance and stable inverted polymer solar cells. *Advanced Materials*, 24(38): 5267-5272.
- Yu, H., Bai, Y., Zong, X., Tang, F., Lu, G. M., and Wang, L. (2012a). Cubic CeO<sub>2</sub> nanoparticles as mirror-like scattering layers for efficient light harvesting in dye-sensitized solar cells. *Chemical Communications*, 48(59): 7386-7388.
- Yu, L., Liu, Z., Liu, S., Hu, X., and Liu, L. (2009). Fading spectrophotometric method for the determination of polyvinylpyrrolidone with eosin Y. *Chinese Journal of Chemistry*, 27(8): 1505-1509.
- Yu, S.-H., Cölfen, H., and Fischer, A. (2004). High quality CeO<sub>2</sub> nanocrystals stabilized by a double hydrophilic block copolymer. *Colloids and Surfaces A: Physicochemical and Engineering Aspects*, 243(1-3): 49-52.
- Yu, X. Y., Xu, R. X., Gao, C., Luo, T., Jia, Y., Liu, J. H., and Huang, X. J. (2012b). Novel 3D hierarchical cotton-candy-like CuO: surfactant-free solvothermal synthesis and application in As (III) removal. *ACS applied materials and interfaces*, 4(4): 1954-1962.
- Zamaro, J. M., Pérez, N. C., Miró, E. E., Casado, C., Seoane, B., Téllez, C., and Coronas, J. (2012). HKUST-1 MOF: a matrix to synthesize CuO and CuO–CeO<sub>2</sub> nanoparticle catalysts for CO oxidation. *Chemical engineering journal*, 195: 180-187.
- Zarinkamar, M., Farahmandjou, M. and Firoozabadi, T. P. (2016). One-step synthesis of ceria (CeO<sub>2</sub>) nano-spheres by a simple wet chemical method. *Journal of Ceramic Processing Research*, 17(3): 166-169.

- Zeng, S., Zhang, W., Guo, S., and Su, H. (2012). Inverse rod-like CeO<sub>2</sub> supported on CuO prepared by hydrothermal method for preferential oxidation of carbon monoxide. *Catalysis Communications*, 23: 62-66.
- Zhai, T., Li, L., Wang, X., Fang, X., Bando, Y. and Golberg, D. (2010). Recent Developments in One-Dimensional Inorganic Nanostructures for Photodetectors. *Advanced Functional Materials*, 20(24): 4233-4248.
- Zhang, H., Wang, W., Zhang, B., Li, H. and Zhang, Q. (2016). Controllable synthesis of spherical cerium oxide particles. *RSC Advances*, 6(37): 30956-30962.
- Zhang, J., Liu, J., Peng, Q., Wang, X. and Li, Y. (2006). Nearly monodisperse Cu<sub>2</sub>O and CuO nanospheres: preparation and applications for sensitive gas sensors. *Chemistry of materials*, 18(4): 867-871.
- Zhang, Q., Zhang, K., Xu, D., Yang, G., Huang, H., Nie, F., Liu, C. and Yang, S. (2014). CuO nanostructures: Synthesis, characterization, growth mechanisms, fundamental properties, and applications. *Progress in Materials Science*, 60: 208-337.
- Zhang, W., Wang, H., Zhang, Y., Yang, Z., Wang, Q., Xia, J. and Yang, X. (2013). Facile microemulsion synthesis of porous CuO nanosphere film and its application in lithium ion batteries. *Electrochimica Acta*, 113: 63-68.
- Zhang, X., Wang, G., Liu, X., Wu, J., Li, M., Gu, J., Liu, H. and Fang, B. (2008a). Different CuO nanostructures: synthesis, characterization, and applications for glucose sensors. *The Journal of Physical Chemistry C*, 112(43): 16845-16849.
- Zhang, X., Wang, G., Zhang, W., Hu, N., Wu, H. and Fang, B. (2008b). Seed-mediated growth method for epitaxial array of CuO nanowires on surface of Cu nanostructures and its application as a glucose sensor. *The Journal of Physical Chemistry C*, 112(24): 8856-8862.
- Zhang, X., Zhang, D., Ni, X. and Zheng, H. (2008c). Optical and electrochemical properties of nanosized CuO via thermal decomposition of copper oxalate. *Solid-State Electronics*, 52(2): 245-248.
- Zheng, N. and Stucky, G. D. (2006). A general synthetic strategy for oxide-supported metal nanoparticle catalysts. *Journal of the American Chemical Society*, 128(44): 14278-14280.
- Zheng, X., Zhang, X., Wang, X., Wang, S. and Wu, S. (2005). Preparation and characterization of CuO/CeO<sub>2</sub> catalysts and their applications in low-temperature CO oxidation. *Applied Catalysis A: General*, 295(2): 142-149.

Zhou, K., Wang, R., Xu, B. and Li, Y. (2006). Synthesis, characterization and catalytic properties of CuO nanocrystals with various shapes. Nanotechnology, 17(15): 3939.

